AD-A154 656 THE SHEARING CONTRIBUTION IN TRANSFORMATION TOUGHENING OF BRITTLE MATERIALS(U) ILLINOIS UNIV AT URBANA DEPT OF THEORETICAL AND APPLIED MECHANICS P SOFRONIS ET AL. 1/1

UNCLASSIFIED MAR 85 N00014-81-K-0650 F/G 20/12 NL

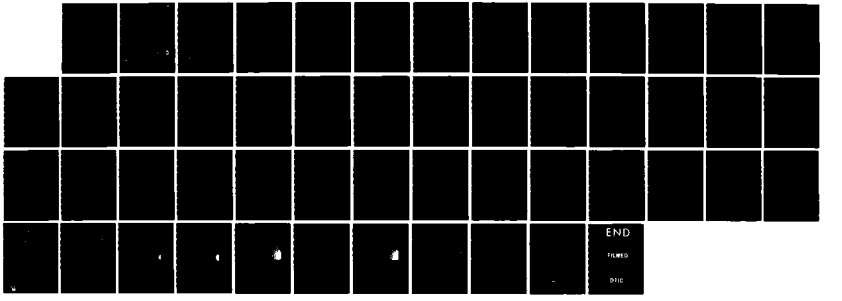

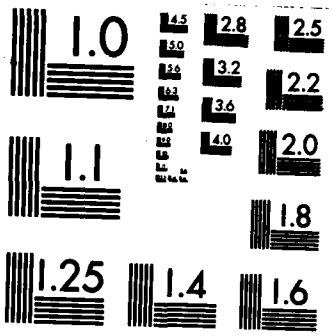

Contract N00014-81-K-0650

The Shearing Contribution in Transformation Toughening of Brittle Materials

P. Sofronis and R. M. McMeeking

Department of Theoretical and Applied Mechanics

University of Illinois at Urbana-Champaign

March 1985

SUMMARY

A simple constitutive law is proposed for the description of a ceramic composite which undergoes stress induced martensitic transformation. This law is used in finite element calculations to investigate the shear effect on the transformation zone near a crack tip. A formula describing the stress intensity factor change due to the shear contribution of the transformation is given. Significant loss of toughness is observed in the case of a stationary crack and is attributed entirely to the shear component of the transformation. ~~On the contrary, the dilatant part brings about no change.~~ As the crack grows, the wake of the transformed material left behind the crack constitutes a source of toughening. This toughening is due to both dilatancy and shear in the phase change and rises to a maximum level just after a propagation comparable with the zone height. Finally, it is shown that the shear component can be important when prediction of the fracture toughness of the transformation toughened ceramics are made.

1. INTRODUCTION

Transformation toughening is one of the mechanisms available to overcome the inherent brittleness of ceramics. It is a phenomenon applicable to ceramic matrices in which Zirconia (ZrO_2) and perhaps some other materials can be incorporated. To date it has been studied quite thoroughly [1-13].

An optimally-fabricated [13] partially stabilized zirconia (PSZ) is a two-phase ceramic. Its microstructure [5] at room temperature consists of: a cubic matrix which is a high solute content Zirconia 'alloy' containing one of the stabilizers MgO CaO, Y_2O_3 or any of the rare earth oxides: and fine coherent metastable tetragonal precipitates of low solute content Zirconia phase inside the cubic matrix. The stress induced martensitic transformation of those metastably retained tetragonal particles to monoclinic symmetry in the stress field of a crack tip is the mechanism responsible for the enhanced toughness observed experimentally in PSZ. The phenomenon of transformation toughening is also observed in the Al_2O_3 and ZrO_2 system. The pure tetrogonal ZrO_2 particles are retained metastably in the Al_2O_3 matrix by pressure.

There are two methods of analysis with regard to the phenomenon of toughening. The first incorporates the energy changes accompanying the transformation. The second concerns the stress intensity factor (SIF) changes that take place during transformation.

Quantitative analysis from a continuum mechanics viewpoint, based only on the dilatational component of the transformation with regard to the SIF reduction was done first by McMeeking and Evans [19] and Budiansky, Hutchinson and Lambropoulos [20]. The analysis of the latter workers is based on a constitutive relation between the mean stress and the dilatation for the composite ceramic. In both works mentioned, the predicted toughening is comparable with the experimental data, however, it underestimates them.

Recently, Lambropoulos [21] has suggested a promising constitutive law for the composite including both parts of the transformation, dilatant and shear. The treatment of the shear effect takes into consideration particle size and orientation. The results predicted for spherical particles are quite well in agreement with experimental observations but are based on a transformation zone size and shape estimated from the standard crack tip singular elastic field. That is, he assumes that the zone shape is the same as regions in the unperturbed elastic solution in which the transformation criterion is met or exceeded. Changes in stress due to the transformation are not addressed in detail.

In this paper, we shall study the shear effect's influence on the enhanced toughness through numerical calculations by means of a simple stress-strain relation for the composite. The model is based on a constitutive relation along the lines introduced by Budiansky *et al.* [20] and the condition for transformation is dominated by the dilatational component. When the hydrostatic stress reaches a critical level, the transformation takes place. This model is not entirely satisfactory as the shear effect is bound to influence the critical state for transformation. However, we regard this paper with the critical state determined solely by the hydrostatic stress as a first step towards a complete theory. The analysis is carried out around the crack tip of a long crack which is imbedded in a composite material rich in tetragonal particles whose presence in the matrix is defined by a volume concentration v_f. As such, the composite can be modelled as a continuum of transformable material.

In section 2 we discuss some aspects of the shear part of the transformation which are helpful in comprehending the nature of the shear strain that the transforming particles undergo. In section 3 we propose a

constitutive law for the composite. In section 4 we derive a formula for the SIF change due to the shear component of the transformation. Based on that formula, we make first estimates of the shearing contribution to SIF change by using the transformation zone derived from the unperturbed elastic solution [19]. In section 5 we formulate the boundary value problem for the stationary crack and solve it by means of the finite element method in section 6. As a result the transformation zone shape and size are estimated. In section 7 the estimated zone and the fracture toughness calculations for the stationary and for the propagating crack are presented. As it has already been proven in the past, the toughness increase is due to the transformed particles left in the wake of the crack tip. In sections 8 and 9 the discussion associated with the model results and the closure are presented respectively.

2. STRESS INDUCED TRANSFORMATION

The aim of this section is to introduce basic features of the stress induced transformation so that the shear component can be understood. The transformation is martensitic and has been discussed extensively elsewhere [1,16,17,18]. It involves a change from tetragonal to monoclinic symmetry in particles in the composite ceramic. In the situation of interest to us, the transformation is induced by critical conditions of stress. A component of the transformation is a dilatation and if the particles were unconstrained there would also be a substantial shear contribution. If we assume that the process is driven by the reduction of free energy [1,7,13] then we deduce that the shear strain component of the transformation would align itself to maximize the work done by the loads applied to the particle [7,13]. In addition, the critical state for transformation would arise just when the applied loads are capable of delivering sufficient energy to the system to

compensate for the increase in the internal energy [7,13]. This implies a transformation criterion involving some combination of hydrostatic and deviatoric stress. This issue has been addressed by Lambropoulos [21].

It has been observed that the situation is more complicated when the transforming particles are constrained in the composite matrix [12]. The particles are capable of twinning or undergoing some similar mode of deformation during transformation. The twins form in such a way that the average shear strain after transformation can be quite small compared with the potential unconstrained shear transformation strain. In addition, the final strain in the transformed particle differs because of the constraint of the surrounding matrix. There is not yet a comprehensive theory that accounts for transformation and twinning. However, it can be hypothesized that the orientation of the net shear strain that results from transformation and twinning will be aligned with the maximum shear stress applied by the matrix to the particle. This will tend to maximize the external energy absorption during transformation and suggests a critical state for the transformation based on strain energy. Lambropoulos [21] has developed a constitutive law for the constrained transformation along the above lines combining the effects of hydrostatic and deviatoric stress and accounting for dilatational and shear transformation.

In this paper we shall use a simpler law as a first step towards studying the interactions of shear transformation with the crack tip. The process will be considered to take place on a continuum scale and the description of the constitutive law applies to the composite ceramic. The criterion for transformation will be taken to be the achievement of a critical average hydrostatic stress in the composite. This neglects the contribution made by the shear component to the work absorbed during transformation. However, the

residual shear strains in constrained transformation particles are known to be small and the shear strain in an unconstrained composite element would be correspondingly small. The transformation will involve a deviatoric component as well as a dilatational contribution. The deviatoric part of the transformation strain for an unconstrained element of the composite ceramic will be taken to be proportional to the dilatational component of the unconstrained transformation. All calculations presented in this paper will be for plane strain situations. In that case there is a fixed ratio between the shear strain and the volumetric strain in the transformation. The orientation of the shear strain will be taken as that of the maximum shear stress when transformation commences (fig. 1). Once the transformation has taken place this orientation will be locked in so that changes of direction of the maximum shear stress will not cause rotation of the shear contribution of the transformation.

Finally, the transformation will be supercritical in the terminology of Budiansky et al. [20]. That is, at critical state, the material transforms completely without the existence of a partially transformed state. The details of the constitutive law are given in the next section.

3. THE CONSTITUTIVE LAW

The transformation of the composite occurs due to the martensitic transformation of the particles. It takes place when the macroscopic average stress in the composite is such that

$$\sigma_m = \sigma_m^{cr} \tag{1}$$

where $\sigma_m = \frac{\sigma_{kk}}{3}$ is the mean stress, σ_m^{cr} is a critical value and σ_{ij} is the macroscopic average stress tensor at a point in the composite.

The unconstrained transformation strain of the composite is ε_{ij}^T which is partly dilatational and partly deviatoric in general. It can be estimated to be the volume fraction v_f of particles in the composite times the unconstrained transformation strain of the transforming particles less the deviatoric strain nullified by twinning [20]. The supercriticality of the transformation implies that there is no transformation as long as $\sigma_m < \sigma_m^{cr}$ and complete transformation occurs if $\sigma_m \geq \sigma_m^{cr}$. The transformation will be assumed to be effectively irreversible in the conditions prevailing as observed in experiment [19]. The amount of the deviatoric strain arising during transformation is proportional to the amount of dilatation. We will carry out calculations for a variety of values of this ratio. The principal axes of the deviatoric strain will be taken to depend on the state of stress at transformation as discussed below.

The stress which arises [22] in a constrained element of the composite is

$$\sigma_{ij} = c_{ijk\ell} (\varepsilon_{k\ell} - \varepsilon_{k\ell}^T) \tag{2}$$

where ε_{ij} is the final strain and $c_{ijk\ell}$ is the tensor of linear elastic moduli of the composite material. For an isotropic composite

$$\sigma_{ij} = 2\mu (e_{ij} - e_{ij}^T) + B(\varepsilon_{kk} - \varepsilon_{kk}^T)\delta_{ij} \tag{3}$$

where μ is the shear modulus, B is the bulk modulus, $e_{ij} = \varepsilon_{ij} - \frac{1}{3} \varepsilon_{kk} \delta_{ij}$ is the deviatoric strain, δ_{ij} is the Kronecker delta and ε^T is the dilatational part of the unconstrained transformation of the composite ($\varepsilon^T = \varepsilon_{kk}^T$).

The calculations we have carried out are for plane strain. In this case $\varepsilon_{zz} = 0$ and we assume that $e_{zz}^T = 0$ as there are no macroscopic transverse shear strains. As a consequence

$$\sigma_{zz} = \nu(\sigma_{xx} + \sigma_{yy}) - \frac{2}{3}\mu(1 + \nu)\,\varepsilon^T \qquad (4)$$

where ν is the poisson's ratio. The deviatoric transformation strain can be written as

$$e^T_{xx} = -e^T_{yy} = -\frac{\gamma^T}{2}\sin 2\Omega, \qquad e^T_{xy} = \frac{\gamma^T}{2}\cos 2\Omega$$

where Ω is the angle between the x-axis and a principal axis of the transformation shear. Thus, the transformation is determined by 3 parameters ε^T, γ^T and Ω. We will assume that Ω is coincident with the angle to the principal axes of shear stress in the macroscopic composite state of stress at the instant of transformation as shown in fig. 1. Calculations are carried out for a variety of ratios $\lambda = \gamma^T/\varepsilon^T$.

4. ESTIMATES OF THE SHEARING EFFECT AT THE CRACK TIP

Before proceeding to somewhat rigorous numerical calculations, we shall consider some approximate results for shearing transformation at the crack tip. The shape of the zone of transformed material at the crack tip is determined by the interaction of the stresses generated by the applied load and those generated by constraints on the transformed zone. If we neglect the latter, we can estimate the zone shape as the locus of points at critical state in the unperturbed linear elastic solution at the crack tip. This proves to be quite an accurate estimate of shape for the case of small scale dilatant transformation [20]. As we have approximated the critical state as one that depends only on hydrostatic stress, the zone shape will be given by the locus of points of equal hydrostatic stress. We will restrict ourselves to small scale transformation, so that the stresses of interest are given by the singular elastic stresses at the crack tip due to the applied load

$$\sigma_{ij} = \frac{K_A}{\sqrt{2\pi r}} f_{ij}(\theta) \tag{5}$$

where K_A is the stress intensity due to the applied loads causing tensile opening (Mode I) of the tip, (r,θ) are polar coordinates measured from the crack tip and f_{ij} is a given function which can be found for example in the article by Rice [24]. The shape that results for a stationary crack is shown in fig. 2.

Consider now, the material which transforms inside the zone. If it were not constrained by the material outside the zone, a certain change of shape would result. Tractions can be applied to the perimeter of this region of material to return it exactly to the shape of the zone prior to transformation. After the material is inserted into the crack tip location, the tractions can be removed to give the final state. However, the forces required to nullify the constraining tractions $\underline{T}^C$ will produce a change in the SIF at the crack tip. It is this change of stress intensity ΔK which is of interest.

As discussed by McMeeking and Evans [19] the change of stress intensity is given by

$$\Delta K = \int_{S_T} \underline{T}^C \cdot \underline{h} \, ds \tag{6}$$

where $\underline{h}$ is the weight function [25] whose form is stated in McMeeking and Evans [19] and used with the assumption that ε_{ij}^T is homogeneous in A_T, the transforming area which has perimeter S_T. We shall consider now transformations which are inhomogeneous $\varepsilon_{ij}^T(\underline{x})$. With the area A_T removed from constraint of the surrounding area, the displacements and strains [22] that result will be $\underline{u}^S$ and $\underline{\underline{\varepsilon}}^S$ respectively due to transformation and self-

constraint within A_T. This will give rise to an elastic stress such that

$$\sigma^S_{ij} = C_{ijk\ell}\,(\varepsilon^S_{k\ell} - \varepsilon^T_{k\ell})$$

$$\sigma^S_{ij,i} = 0 \qquad \text{in} \quad A_T \tag{7}$$

$$n_i\,\sigma^S_{ij} = 0 \qquad \text{on} \quad S_T$$

where $\underline{n}$ is the unit outward normal to S_T and $\sigma^S_{ij,i} = \dfrac{\partial \sigma^S_{ij}}{\partial x_i}$ with x_i denoting position in a fixed cartesian coordinate system. Tractions are now applied around A_T producing further displacements $\underline{u}^R$ and strains $\underset{\sim}{\varepsilon}^R$ so that A_T has its original shape prior to transformation. As a result

$$\sigma^R_{ij} = C_{ijk\ell}\,(\varepsilon^R_{k\ell} + \varepsilon^S_{k\ell} - \varepsilon^T_{k\ell}) \tag{8a}$$

$$\sigma^R_{ij,i} = 0 \qquad \text{in} \quad A_T \tag{8b}$$

$$u^R_i + u^S_i = 0 \qquad \text{on} \quad S_T. \tag{8c}$$

Using σ^R_{ij} we can express $\underline{T}^c$ as follows

$$T^c_j = -\,n_i\,\sigma^R_{ij}$$

Thus, equation (6) becomes

$$\Delta K = -\int_{S_T} n_i\,\sigma^R_{ij}\,h_j\,ds$$

As noted by Rice [25], $\underline{h}$ can be treated as a displacement and so by the

principle of virtual work

$$\Delta K = -\int_{A_T} \sigma_{ij}^R \, h_{j,i} \, ds \tag{9}$$

Substitution of (8a) into (9) furnishes

$$\Delta K = \int_{A_T} (\varepsilon_{ij}^T - \varepsilon_{ij}^R - \varepsilon_{ij}^S) \, C_{ijk\ell} \, h_{\ell,k} \, dA \tag{10}$$

As further noted by Rice [25] $C_{ijk\ell} \, h_{\ell,k}$ is a stress field in equilibrium in A_T because $\underline{h}$ is related to the difference between two displacement fields each possessing equilibrium stress fields. This means that the virtual work principle can be used to show

$$\int_{A_T} (\varepsilon_{ij}^R + \varepsilon_{ij}^S) \, C_{ijk\ell} \, h_{\ell,k} \, dA_T = \int_{S_T} n_i \, C_{ijk\ell} \, h_{\ell,k} (u_j^R + u_j^S) \, dS$$

$$= 0 \quad \text{due to (8c)}$$

This means that equation (10) is written as

$$\Delta K = \int_{A_T} \varepsilon_{ij}^T \, C_{ijk\ell} \, h_{\ell,k} \, dA_T \tag{11}$$

For isotropic material, equation (11) becomes

$$\Delta K = \Delta K_D + \Delta K_S \tag{12a}$$

where $\Delta K_D = B \int_{A_T} \varepsilon^T \, h_{k,k} \, dA$ (dilatational contribution) (12b)

$\Delta K_S = 2\mu \int_{A_T} e_{ij}^T \, h_{i,j} \, dA$ (shearing contribution) (12c)

iv) experimentally measured value

$$\Delta K = -2.3 \quad \text{MPa}\sqrt{\text{m}} \quad (\text{implies } \lambda \simeq 3)$$

The preceding toughness enhancement calculations should be regarded tentative because of the uncertainties involved in the material parameters. Nevertheless, it is clear that the predicted toughness increase may be in agreement with the experimental data when the shearing contribution is considered in the transformation mechanism analysis. An important role is played by the parameter λ which determines the amount of the shearing contribution. We have arbitrarily used 1 because we have no information on what values may be realistic. Alternately, we can compute a value of λ necesssary to bring our estimates into agreement with the experimental values. These are the implied values of λ listed. Some of these values are rather large. However, the amount of shear strain during transformation is typically quite large compared to the dilatation. Even if substantial amounts of this are nullified by twinning, this could still leave values of λ of the order implied.

9. CLOSURE

For further and more elaborate treatment of the shear effect one may need to incorporate size and particle orientation effects via a more realistic constitutive law for the composite. This must include a consideration of the effect of twinning during the transformation. However, our simple calculations have indicated that shear strain effects may be significant and that further work on the mechanics of the phenomenon may be profitable.

$$\Delta K = -1.70 \quad \text{MPa}\sqrt{m}$$

iv) experimentally measured value

$$\Delta K = -2.4 \quad \text{MPa}\sqrt{m} \text{ (implies } \lambda \simeq 1.7)$$

For another system whose the parameters are [21]: E = 470 GPa, $\varepsilon^T = 0.04$ w = 5.10^{-6}m, $v_f = 0.3$ one has

i) with purely dilatant transformation

$$\Delta K = -3.96 \quad \text{MPa}\sqrt{m}$$

ii) with both parts of the transformation and $\lambda = 1$

$$\Delta K = -6.30 \quad \text{MPa}\sqrt{m}$$

iii) Lambropoulos' result (both parts of the transformation, spherical particles and $K_{IC} = 6$ MPa $\sqrt{m}$)

$$\Delta K = -4.5 \quad \text{MPa}\sqrt{m}$$

iv) experimentally measured value

$$\Delta K = -6 \quad \text{MPa}\sqrt{m} \text{ (implies } \lambda \simeq 0.9)$$

In the case of the MgO partially stabilized Zirconia whose parameters are [19]: E = 200 GPa, $\varepsilon^T = 0.058$, w = 6.10^{-6}m, $v_f = 0.3$ one has:

i) with purely dilatant transformation

$$\Delta K = -0.85 \quad \text{MPa}\sqrt{m}$$

ii) with both parts of the transformation and $\lambda = 1$

$$\Delta K = -1.35 \quad \text{MPa}\sqrt{m}$$

iii) Lambropoulos' result (both parts of the tranformation, spherical particles and $K_{IC} = 1.97$ MPa $\sqrt{m}$)

$$\Delta K = -1.04 \quad \text{MPa}\sqrt{m}$$

sufficient in general to consider only the effect of very long wakes that produce an asymptotic value for ΔK.

For λ less than 1 the toughness enhancement is not as large as that given by equation (18). In table 5 we present the greatest toughness enhancements found for several λ values and the amount of crack advance for which they were obtained. This table shows that the toughness enhancement gets larger when λ gets larger. It should be mentioned that the values for ΔK tend to certain asymptotic values as $\Delta a/w \to \infty$ but these are less important than the maxima presented in table 5. Finally, we should mention the fact that the results of table 5 fit the curve for $\nu = 0.25$ of figure 4. This means that the results taken in section 4 and those after having solved the boundary value problem of the stationary crack are the same.

Applications

Next, we proceed to see how the maximum toughness enhancement results compare with the experimental data. We shall consider $\nu = 0.3$ even though our shearing contribution results have been taken by considering $\nu = 0.25$. Figure 4 indicates that no significant difference results. In the case of the Al_2O_3 toughened Zirconia whose material and transformation parameters are [21]: $E = 315$ GPa, $\varepsilon^T = 0.04$, $w = 10^{-6}$m, $v_f = 0.03$ one has

i) with purely dilatant transformation

$$\Delta K = -1.19 \quad \text{Mpa} \sqrt{\text{m}}$$

ii) with both parts of the transformation and $\lambda = 1$

$$\Delta K = -1.89 \quad \text{MPa} \sqrt{\text{m}}$$

iii) Lambropoulos' result (both part of the transformation, spherical particles and $K_{IC} = 5$ MPa $\sqrt{\text{m}}$)

based on equation (16). Such "R curves" are those shown in figures 12 and 13 for $\lambda = 0$ and $\lambda = 1$ respectively. Observing those curves and the tables 2 through 4 we deduce that the wake of the transformed material left behind the propagating crack is a source of fracture toughness enhancement. First, figure 12 shows that the toughness enhancement found for $\lambda = 0$ coincides with that found by McMeeking and Evans [19]. This coincidence becomes more pronounced for large values of crack advance.

The important result of this paper is the ΔK_S component that behaves as for examaple figure 13 shows for $\lambda = 1$. As mentioned previously, the crack will start to propagate sooner than in the absence of transformation because ΔK is initially positive due to ΔK_S. As the crack grows, ΔK diminishes and eventually becomes negative at about $\Delta a/w = 0.1$. This means that the applied loads must be increased to sustain crack growth and in a stiff loading system the crack will propagate stably under rising load. This will continue until $\Delta a/w$ is about 0.7 and the SIF change is then given by

$$\frac{(1-\nu)\ \Delta K}{E\ \varepsilon^T\ v_f\ \sqrt{w}} = -\ 0.35. \qquad (23)$$

This expression represents the toughness enhancement and is larger than that given by equation (18). After this amount of crack growth, ΔK increases and so if the loads are kept constant or increased, the applied K will exceed K_{IC}. Thereafter the propagation will become unstable. Thus the maximum magnitude of ΔK represented by equation (23) is equivalent to the asymptotic value of ΔK due to dilatation alone observed by McMeeking and Evans [19]. It is interesting to note that the asymptotic value of ΔK due to dilatation plus shear is not the relevant quantity. The useful toughness enhancement is due to the minimum in the curve for ΔK at $\Delta a/w \simeq 0.7$. Thus it may not be

been extended to the cases when $\lambda \neq 0$.

In contrast with ΔK_D, ΔK_S is not zero and it does depend on the value of λ. In fact, ΔK_S increases as λ increases. Equation (16) indicates that the shearing effect results in fracture toughness reduction because ΔK_S is positive. This reduction for $\lambda = 1$ is comparable to the fracture toughness enhancement in the case of a purely dilatant transformation given by equation (18) when the crack has advanced $\Delta a = 5w$. The ΔK_S results in table 1 can almost be reproduced by the equation (17) for the respective values of λ. This means that the transformed material and the shearing contribution do not affect the features of the transformation zone as it is found from the unperturbed elastic crack tip field. Therefore, the fact that ΔK_S is positive is a consequence of the nature of the equation (16). An attempt to justify this may be made by regarding the range of the positive contribution to the integral of equation (16). Since for the stationary crack $\Omega = \frac{3\theta}{4}$, the integral sign depends on the sign of the integrand $\sin(2\theta)$. Hence, it is positive when $\theta < \frac{\pi}{2}$ and negative when $\theta > \frac{\pi}{2}$. Therefore, it can be said that the positive contribution comes from a large sector and can very likely override the negative contribution.

The consequence of the computed ΔK_S values would be that crack propagation may take place sooner than when there is no transformation. This is because ΔK_S is positive for the stationary crack and K_A can become greater than K_{IC}^A earlier than otherwise. However, this growth is likely to be stable, a point which is elucidated in what follows.

Propagating crack

In order for the crack to advance quasi-statically it is required that the applied loads K_A be such that $K_A = K_{IC}^A$ where K_{IC}^A is given by equation (16). Therefore, by knowing ΔK , we can produce an "R curve" [15]

zones are developed inside a circle centered at the crack tip whose area is less than 0.15% of the mesh. Indeed, these numbers fall within the corresponding length range, set for small scale yielding condition in the elastic-plastic fracture analysis by Rice and Tracey [23]. In addition, the fact that the displacements of the elements near the perimeter of the domain (fig. 5) are the unperturbed elastic crack tip field displacements, ensures the small scale condition too. In figure 9, it can be seen that the zone taken numerically for $\lambda = 0$ is almost identical with that used by McMeeking and Evans [19] as predicted by Budiansky et al. [20]. This means that the transformed material does not affect the linear elastic crack tip field given by equation (5). The same argument applies to the case when $\lambda = 1$ (fig. 11). However, the shearing contribution affects the zone shape especially at small angles of θ. It is also worth mentioning that the zone height w is the same for all values of λ as shown in table 1.

Consider now the SIF change ΔK_D. It can be deduced from table 1 that $\Delta K_D = 0$ if we take into account the numerical error involved in the calculations. Therefore, for $\lambda > 0$ no ΔK_D is observed even though the zone boundaries differ from that with $\lambda = 0$. This independence of ΔK_D from λ can be justified by observing equation (13). The sign of the integral depends on the sign of the $\cos(\frac{3\theta}{2})$. The integral is positive for $\theta < \frac{\pi}{3}$ and negative for $\theta > \frac{\pi}{3}$. Thus, the positive contribution to the integral value comes from a much smaller section than the sector of the negative contribution. It is this wider ranging source of the negative effect which dominates the integral value. Therefore, the larger range of r for small θ when λ deviates from zero cannot be cause of a significant disturbance of the final result. This remark has already been made before [19], but only within the frame of a purely dilatant transformation. The argument now has

Propagating crack

The crack has been assumed to propagate quasi-statically under the conditions mentioned in section 4. The SIF change calculations ΔK_D and ΔK_S were carried out numerically for a given crack advance Δa. The formulae (13) and (14) were used again. The results are shown in tables 2 through 4. In figures 12 and 13 the changes ΔK_D and ΔK_S are plotted against the crack advance Δa for $\lambda = 0$ and $\lambda = 1$ respectively. In table 5 the symptotic, i.e. the maximum SIF change $\Delta K = \Delta K_D + \Delta K_S$ is shown.

8. DISCUSSION

In this discussion of the results quoted in the previous section, we shall focus mainly on how the shear component of the transformation influences the fracture toughness behavior of the material. It should be borne in mind that the shearing contribution is characterized by the parameter $\lambda = \gamma^T/\varepsilon^T$. Large values of λ denote large transformation shear strains for a given volume dilatation.

Stationary crack

It has been mentioned before that the dilatant part of the transformation does not affect the material fracture toughness, i.e. $\Delta K_D = 0$. Furthermore, Lambropoulos [21] based on a transformation zone derived from the unperturbed linear elastic crack tip field, concluded that $\Delta K_S = 0$ too. Our analysis' predictions are in accord with the above results only as far as ΔK_D is concerned. Table 1 shows that ΔK_S is not zero. However, we have used a different constitutive law from Lambropoulos.

Before discussing the nature of ΔK_D and ΔK_S we should emphasize that the small scale transformation condition is satisfied. This is because the

Stationary crack

The transformation zone for $\lambda = 0$ is shown in fig. 8. There is no shearing effect because $\gamma^T = 0$. The asterisks indicate the element integration stations where the condition for transformation was met. The transformed zone covers an area only 0.1% of the mesh. The nodal displacements of the elements near the external boundary of the domain (fig. 5) are identical within 3 significant figures to the linear elastic ones when transformation does not take place. The periphery of the transformation zone is shown in fig. 9. The curve denoted by the letter D is the periphery of the transformation zone used by McMeeking and Evans [19]. This last zone is given by $r = \frac{8}{3\sqrt{3}} w \cos^2(\frac{\theta}{2})$ where the height w has been taken to agree with the height of the finite element zone.

The transformation zone for $\lambda = 1$ is shown in fig. 10. The boundary of the zone is shown in fig. 11 along with the zone used by McMeeking and Evans as described before. The zones have the same height as the zone for $\lambda = 0$. However, its leading front appears to be elongated along the x axis as $y \to 0$ compared to the other zone. As a result, an inflection point is observed. The zone boundary to the left of this point tends to be concave whereas the boundary to the right tends to be convex. It is worth noting that this tendency for elongation increases with increasing values of λ. This observation has been confirmed by the appearance of the zone boundaries that we generated for intermediate values of λ.

The SIF change calculations were carried out numerically by using the formulae (13) and (14) for the ΔK_D and ΔK_S changes respectively. These changes are shown in Table 1.

where [C] is the linear elastic stress-strain matrix for plane strain, for the composite, $\{T\}$ is the two-dimensional traction vector, $\{u_N\}$ is the nodal displacements and $\{E_T\}$ is the element transformation strain vector given by

$$\{E_T\} = \begin{matrix} \frac{2(1+\nu)}{3(1-2\nu)}\,\varepsilon^T - \gamma^T \sin 2\Omega \\ \frac{2(1+\nu)}{3(1-2\nu)}\,\varepsilon^T + \gamma^T \sin 2\Omega \\ \gamma^T \cos 2\Omega \end{matrix} \qquad (22)$$

It is worth noting that the stiffness matrix [K] is independent of the transformation since it involves only the elasticity tensor [C] and the interpolation matrix [B]. The same is true for the vector $\{F_b\}$. However, the quantity $\{F_T\}$ depends on the transformation through $\{E_T\}$.

An iterative method was used to solve equations (21) as stated in section 5. All calculations were carried out for Poisson's ratio $\nu = 0.25$. Solutions were obtained for λ equal to 0, 0.25, 0.5, 0.75 and 1. Extremely rapid convergence was achieved with 3 iterations when the computed displacements were found to converge to within 3 significant figures.

7. RESULTS

In this section we shall discuss the results of the finite element analysis for the stationary crack problem. We shall also give the SIF changes for both stationary crack and quasi-statically advancing crack deduced through a model for that case. The shape and features of the transformation zone for the propagating crack are determined as discussed in section 4 starting from the stationary crack zone. However, the stationary crack zone is now the one deduced via the finite element calculations.

$$\int_A \varepsilon_{k\ell}\, C_{ijk\ell}\, \delta\varepsilon_{ij}\, dA = \int_S T_i\, \delta u_i\, ds + \int_A \varepsilon^T_{k\ell}\, C_{ijk\ell}\, \delta\varepsilon_{ij}\, dA \qquad (20)$$

Equation (20) illustrates the nonlinearity of the problem. That is, the second integral on the right hand side can only be determined after the solution is found. Thus, the solution procedure will involve iteration. Assuming a solution we determine the transformation zone. Next, we solve the resulting linear problem arising from equation (20) with the second integral on the right hand side evaluated and compare the solution with the assumed one. The process continues until convergence is achieved. The linear elastic solution can be used to initiate the process with $\varepsilon^T = 0$ i.e. with no transformed region. This method is addressed in detail in the next section.

6. FINITE ELEMENT CALCULATIONS

The finite element method was used to solve the boundary value problem as stated in the previous section. The domain (fig. 5) was discretized into 554 4-noded quadrilateral isoparametric elements with 4 integration stations. In figures 6 and 7 the 224 element near tip mesh and the 320 element far field mesh are shown respectively. The second mesh surrounds the first one. The fine near tip discretization was used in order to ensure that the transformation zone is determined fairly reliably. By using the standard element displacement and strain interpolation matrices [A] and [B] respectively, we rewrite the governing equation (20) as follows

$$[K]\,\{u_N\} = \{F_b\} + \{F_T\} \qquad (21a)$$

with

$$[K] = \int_A [B]^T\,[C]\,[B]\, dA \qquad \text{(stiffness matrix)} \qquad (21b)$$

$$\{F_b\} = \int_A [A]^T\,\{T\}\, ds \qquad \text{(applied load vector)} \qquad (21c)$$

$$\{F_T\} = \int_A [B]^T\,\{E_T\}\, ds \qquad \text{(transformation load vector)} \qquad (21d)$$

transformation zone appropriately. This is accomplished by taking into account the perturbation of the linear elastic crack field induced by the transformation. This subject is addressed in the next section.

5. THE BOUNDARY VALUE PROBLEM FOR THE STATIONARY CRACK

We are concerned with the stresses and deformations near the tip of a long crack in plain strain. The body is loaded so that only mode I (tensile opening mode) stresses arise at the tip. We are concerned with "small scale transformation" where the transformation zone is confined to a region very close to the crack tip. This can be achieved by imposing tractions on a circular boundary far from the tip in agreement with the standard singular linear elastic solution given by equation (5). Symmetry permits the analysis to be confined to a semi-circular domain as shown in fig. 5. The crack surface is traction free and the symmetry line is free of shear traction and displacements normal to the line.

The governing equations in the plane can be stated by the principle of virtual work in the absence of body forces.

$$\int_A \sigma_{ij}\, \delta\varepsilon_{ij}\, dA = \int_S T_i\, \delta u_i\, ds \qquad (19)$$

where A is the area and S is the perimeter of the domain, T_i the tractions on S and u_i the displacements in A. The symbol δ indicates an arbitrary virtual variation of the quantity it precedes. In addition the stresses are related to the strains by the constitutive law given by equation (2). As a result, the governing equation (19) can be rewritten as follows

function of Δa , the amount of crack propagation. The slope versus Δa decreases continuously and the curve appears to approach an asymptote for large values of Δa. At that stage [19,20]

$$\frac{(1-\nu)\ \Delta K_D}{E\ \varepsilon^T\ v_f\ \sqrt{w}} = -\ 0.22 \qquad (18)$$

To maintain the critical propagation value of $K = K_{IC}$ for the material at the crack tip the loads would have to be increased with Δa. This will mean an apparent higher value of $K = K_A$ computed from the applied loads. The material will appear to be toughened as a result.

Consider now the shearing contribution to ΔK. According to our hypothesis, particles enter the transformation zone ahead of the crack and the direction of shearing transformation will be determined by the state of stress there. We assume still that the stress field is unperturbed by the presence of a zone and so Ω equals to current value of $\frac{3\theta}{4}$ measured from the crack tip. As the crack propagates by, this value of Ω will remain unchanged for that particle. Thus all particles on a line parallel to the crack will have the same value of Ω , except those in the zone created before the crack propagated (fig. 3). The resulting contribution ΔK_S from such a wake zone is negative. The maximum of the absolute value of ΔK_S for all λ is achieved when the crack propagates 0.5w whereas the maximum of the absolute value of ΔK_D as found from equation (18), is achieved at $\Delta a = 5w$. In figure 4 the ratio $|\Delta K_S|_{max}/|\Delta K_D|_{max}$ is shown plotted against the ratio λ. As it is seen, the amount of the shearing contribution to the toughening can become the same as that of the dilatant contribution when λ approaches 1. In conclusion, the importance of the shearing contribution raises the need for a more rigorous estimation. Therefore, it is required that we compute the

Results for stationary crack

In this case, the transformed zone has a perimeter which is the locus of points of equal hydrostatic stress. McMeeking and Evans [19] and Budiansky et al. [20] have shown that $\Delta K_D = 0$ for this case.

As far as the shearing contribution is concerned, Ω is taken to be the angle to the principal shearing direction when the material transformed, i.e. at the edge of the zone then prevailing. The stress state is taken to be the unperturbed linear crack tip field and thus $\Omega = \frac{3\theta}{4}$. As a result

$$\frac{(1-\nu)\ \Delta K_S}{E\ \varepsilon^T\ v_f\ \sqrt{w}} = 0.15\lambda \qquad (17)$$

where w is the height of the transformation zone as shown in fig. 2, λ is the ratio γ^T/ε^T and $\nu = 0.3$. The transformation strain has been rewritten as $v_f\ \gamma_p^T$ where γ_p^T is the unconstrained transformation strain after twinning for an individual particle.

Equations (16) and (17) indicate that the shearing effect causes fracture toughness reduction. This reduction becomes larger as λ increases i.e. the shear strain γ^T increases for a given ε^T. As a consequence, crack propagation may occur more readily than in the absence of transformation.

Results for propagating crack

If the crack propagates quasi-statically and there is no reverse transformation, a wake of transformed material is left along the newly created crack surfaces. This wake will be parallel to the crack surfaces if we assume that the tip propagates at a constant value of K (fig. 3). The dilatant contribution to ΔK due to such a transformed zone has been studied by McMeeking and Evans [19] and has been found to be a monotonically decreasing

McMeeking and Evans [19] have shown that

$$\Delta K_D = \frac{E\,\varepsilon^T}{6\sqrt{2\pi}\,(1-\nu)} \int_{A_T} r^{-\frac{3}{2}} \cos(\tfrac{3\theta}{2})\, dA \qquad (13)$$

where E is the Young's modulus. From the form of the weight function $\underline{h}$ and $\underset{\sim}{e}^T$ it can be deduced that

$$\Delta K_S = \frac{3E\,\gamma^T}{8\sqrt{2\pi}\,(1-\nu^2)} \int_{A_T} r^{-\frac{3}{2}} \cos(2\Omega - \tfrac{3\theta}{2}) \sin\theta\, dA \qquad (14)$$

The fact that $\cos(\frac{3\theta}{2})$ is an even function of θ allows the integral in equation (13) to be computed in the region $0 \leq \theta \leq \pi$ (figures 2,3). The same argument applies to equation (14) because $\gamma^T \sin\theta$ is an even function of θ. That is because both γ^T and $\sin\theta$ are odd functions of θ.

The SIF change ΔK is related to the applied field K_A as follows

$$K_t = K_A + \Delta K \qquad (15)$$

where K_t is the S.I.F. that actually describes the crack tip field when the transformation has taken place. If ΔK is negative equation (15) implies that the stress intensity at the crack tip is lower than that associated with the applied loads. In particular, since the crack propagates when K_t becomes equal to the fracture toughness K_{IC} of the pretransformed material [14] the apparent fracture toughness K_{IC}^A is given by

$$K_{IC}^A = K_{IC} - \Delta K \qquad (16)$$

If ΔK is negative the material appears to be tougher than the pretransformed one.

ACKNOWLEDGEMENT

This research was supported by the Office of Naval Research through Contract NR 064-N00014-81-K-0650 with the University of Illinois.

REFERENCES

1. A. G. Evans and A. H. Heuer: J. Am. Ceram. Soc., 63, 241 (1980).

2. R. C. Garvie, R. H. Hannink and R. T. Pascoe: Nature, 258, 703 (1975).

3. N. Claussen: J. Am. Ceram. Soc., 59, 49 (1976).

4. T. G. Gupta, F. F. Lange and J. H. Bechtold: J. Mater. Sci., 13, 1464 (1978).

5. D. L. Porter, A. G. Evans and A. H. Heuer: Acta Metall., 27, 1649 (1979).

6. D. L. Porter and A. H. Heuer: J. Am. Ceram. Soc., 60, 183 (1977).

7. L. H. Schoenlein and A. H. Heuer: Fracture Mechanics of Ceramics, R. C. Bradt et al., Eds., Plenum Press, Vol. 6, 309 (1983).

8. P. F. Becher and V. J. Tennery: Fracture Mechanics of Ceramics, R. C. Bradt et al., Eds., Plenum Press, Vol. 6, 383 (1983).

9. H. Ruf and A. G. Evans: J. Am. Ceram. Soc., 66, 328 (1983).

10. F. F. Lange: J. Mater. Sci., 17, 225 (1982).

11. M. V. Swain, R. H. Hannink and R. C. Garvie: Fracture Mechanics of Ceramics, R. C. Bradt et al., Eds., Plenum Press, Vol. 6, 339 (1983).

12. A. G. Evans, N. Burlingame, M. Drory and W. M. Kriven: Acta Metall., 29, 447 (1981).

13. A. H. Heuer: Advances in Ceramics, American Ceramics Society, A. H. Heuer and L. W. Hobbs, Eds., Vol. 3, 98 (1981).

14. A. G. Evans: Advances in Ceramics, American Ceramics Society, N. Claussen, M. Ruhle and A. H. Heuer, Eds., Vol. 12, 193 (1984).

15. M. V. Swain and R.H.J. Hannink: Advances in Ceramics, American Ceramics Society, N. Claussen, M. Ruhle and A. H. Heuer, Eds., Vol. 12, 225 (1984).

16. G. K. Bansal and A. H. Heuer: Acta Metall. 20, 1281 (1972).

17. G. K. Bansal and A. H. Heuer: Acta Metall. 22, 409 (1974).

18. G. M. Wolten: J. Am. Ceram. Soc., 46, 418 (1963).

19. R. M. McMeeking and A. G. Evans: J. Am. Ceram. Soc., 65, 242 (1982).

20. B. Budiansky, J. W. Hutchinson and J. C. Lambropoulos: Int. J. Solids Structures, 19, 337 (1983).

21. J. C. Lambropoulos: "Shear, Shape and Orientation Effects in Transformation Toughening". Harvard University Report, Division of Applied Sciences, MECH-55 (July 1984).

22. J. D. Eshelby: Proc. Roy. Soc., A 241, 376 (1957).

23. J. R. Rice and D. M. Tracey: Numerical and Computer methods in structural mechanics, S. J. Fenves et al., Eds. (Academic Press, New York, 1973) 585-623.

24. J. R. Rice: Fracture: an advanced treatice 2, H. Liebowitz, Ed. (Academic Press, New York, 1968) 191-311.

25. J. R. Rice: Int. J. Solids Structures, 8, 751 (1972).

TABLE CAPTIONS

Table 1. Stress intensity factor changes for the stationary crack calculated by the finite element method.

Table 2. Stress intensity factor changes for the propagating crack when $\lambda = \gamma^T/\varepsilon^T = 0$ deduced from the finite element calculations.

Table 3. Stress intensity factor changes for the propagating crack when $\lambda = \gamma^T/\varepsilon^T = 0.5$ deduced from the finite element calculations.

Table 4. Stress intensity factor changes for the propagating crack when $\lambda = \gamma^T/\varepsilon^T = 1$ deduced from the finite element calculations.

Table 5. Maximum fracture toughness changes achieved after the crack has advanced quasi-statically.

Table 1

Stress Intensity Factor Changes for the Stationary Crack

λ	w (zone height)	$\frac{(1-\nu)\,\Delta K_D}{E\,e^T\,v_f\,\sqrt{w}}$	$\frac{(1-\nu)\,\Delta K_S}{E\,e^T\,v_f\,\sqrt{w}}$
0.00	2.14	-0.0085	0.0000
0.25	2.14	-0.0066	0.0381
0.50	2.14	-0.0066	0.0762
0.75	2.14	-0.0049	0.1145
1.00	2.14	-0.0049	0.1527

ΔK_D = Dilatational SIF change

ΔK_S = Shearing SIF change

Table 2

Stress Intensity Factor Changes for the Advancing Crack When $\lambda = 0$

$\frac{\Delta a}{w}$	$\frac{(1-\nu)\,\Delta K_D}{E\,e^T\,v_f\,\sqrt{w}}$	$\frac{(1-\nu)\,\Delta K_S}{E\,e^T\,v_f\,\sqrt{w}}$	$\frac{(1-\nu)\,\Delta K}{E\,e^T\,v_f\,\sqrt{w}}$
0.0	-0.0085	0	-0.0085
0.2	-0.0780	0	-0.0780
0.5	-0.1270	0	-0.1270
0.8	-0.1550	0	-0.1550
1.1	-0.1723	0	-0.1723
2.0	-0.1961	0	-0.1961
3.0	-0.2055	0	-0.2055
4.0	-0.2097	0	-0.2097
5.0	-0.2119	0	-0.2119
7.0	-0.2142	0	-0.2142
10.0	-0.2157	0	-0.2157
15.0	-0.2167	0	-0.2167
20.0	-0.2171	0	-0.2171
30.0	-0.2174	0	-0.2174

$\frac{\Delta a}{w}$ = Dimensionless crack advance

ΔK_D = Dilatational SIF change

ΔK_S = Shearing SIF change

ΔK = Total SIF change

Table 3

Stress Intensity Factor Changes for the Advancing Crack When $\lambda = 0.5$

$\frac{\Delta a}{w}$	$\frac{(1-\nu)\,\Delta K_D}{E\,e^T\,v_f\,\sqrt{w}}$	$\frac{(1-\nu)\,\Delta K_S}{E\,e^T\,v_f\,\sqrt{w}}$	$\frac{(1-\nu)\,\Delta K}{E\,e^T\,v_f\,\sqrt{w}}$
0.0	-0.0066	0.0762	0.0695
0.3	-0.0961	-0.0954	-0.1915
0.6	-0.1362	-0.1057	-0.2419
1.0	-0.1656	-0.0860	-0.2516
2.0	-0.1943	-0.0376	-0.2319
3.0	-0.2037	-0.0312	-0.2348
4.0	-0.2079	-0.0298	-0.2377
5.0	-0.2101	-0.0287	-0.2388
10.0	-0.2139	-0.0268	-0.2407
15.0	-0.2149	-0.0258	-0.2406
20.0	-0.2153	-0.0247	-0.2400
30.0	-0.2156	-0.0230	-0.2386

$\frac{\Delta a}{w}$ = Dimensionless crack advance

ΔK_D = Dilatational SIF change

ΔK_S = Shearing SIF change

(ΔK) = Total SIF change

Table 4

Stress Intensity Factor Changes for the Advancing Crack When $\lambda = 1$

$\frac{\Delta a}{w}$	$\frac{(1-\nu)\,\Delta K_D}{E\,e^T\,v_f\,\sqrt{w}}$	$\frac{(1-\nu)\,\Delta K_S}{E\,e^T\,v_f\,\sqrt{w}}$	$\frac{(1-\nu)\,\Delta K}{E\,e^T\,v_f\,\sqrt{w}}$
0.0	-0.0049	0.1527	0.1479
0.3	-0.0944	-0.1904	-0.2848
0.6	-0.1344	-0.2110	-0.3454
1.0	-0.1638	-0.1718	-0.3356
2.0	-0.1925	-0.0744	-0.2669
3.0	-0.2019	-0.0620	-0.2638
4.0	-0.2061	-0.0592	-0.2653
5.0	-0.2084	-0.0570	-0.2653
10.0	-0.2121	-0.0532	-0.2653
15.0	-0.2131	-0.0512	-0.2643
20.0	-0.2135	-0.0492	-0.2626
30.0	-0.2138	-0.0455	-0.2594

$\frac{\Delta a}{w}$ = Dimensionless crack advance

ΔK_D = Dilatational SIF change

ΔK_S = Shearing SIF change

ΔK = Total SIF change

Table 5

"Asymptotic" Fracture Toughness Changes for the Quasi-Statically Advancing Crack

λ	$\frac{\Delta a}{w}$	$\frac{(1-\nu)\,\Delta K}{E\,e^{T}\,v_f\,\sqrt{w}}$
0.00	5.0	-0.2119
0.25	3.2	-0.2202
0.50	0.9	-0.2527
0.75	0.8	-0.2991
1.00	0.7	-0.3494

$\lambda = \gamma^T/\varepsilon^T$

$\frac{\Delta a}{w}$ = Dimensionless crack advance

ΔK = SIF change

Figure Captions

Fig. 1 a. Direction Ω of the maximum shear stress τ

b. Shape change of an unconstrained transforming element. The shearing direction is along the maximum shear stress direction.

Fig. 2. Transformation zone shape based on critical hydrostatic stress transformation and the unperturbed elastic solution for the stationary crack. The maximum height w of the zone appears at $\phi = 60°$. The shearing direction Ω at transformation is also indicated at an arbitrary point (r,θ).

Fig. 3. Transformation zone shape for the quasi-statically advancing crack. The flank of the zone is parallel to the crack surface and tangent to the leading front of the zone at $\theta = 60°$. The shearing direction of the newly transforming elements is determined by the angle Ω at the leading front of the zone. The initially transformed elements retain their own shearing directions.

Fig. 4. Comparison of the maximum shearing contribution to the toughness enhancement with the maximum dilatant contribution. Those contributions are derived from a zone shape shown in fig. 3 when the crack propagated. The zone for the stationary crack is shown in fig. 1. The ΔK_S is achieved after $\Delta a = 0.5w$ whereas the ΔK_D is achieved after $\Delta a = 5w$.

Fig. 5. Domain and boundary conditions for the boundary value problem for the stationary crack.

Fig. 6. Near tip finite element mesh.

Fig. 7. Far field finite element mesh which surrounds the mesh shown in fig. 6.

Fig. 8. Transformation zone for the stationary crack in the case of purely dilatant transformation ($\gamma^T = 0$) derived by solving the boundary value problem by the finite element method.

Fig. 9. Comparison of the zone boundary of fig. 8 with the zone boundary derived by McMeeking and Evans [19] for the purely dilatational transformation and marked D. (fig. 2).

Fig. 10. Transformation zone for the stationary crack when the unconstrained shear transformation strain is equal to the unconstrained volume dilatation. The zone has been derived by solving the boundary value problem by the finite element method.

Fig. 11. Comparison of the zone boundary of fig. 10 with the zone boundary derived by McMeeking and Evans [19] for the purely dilatational transformation (fig. 2) (D).

Fig. 12. The R-curve predicted from the stress intensity factor analysis in the case of purely dilatational transformation.

Fig. 13. The R-curve predicted from the stress intensity factor analysis in the case when the unconstrained shear transformation strain is equal to the unconstrained volume dilatation.

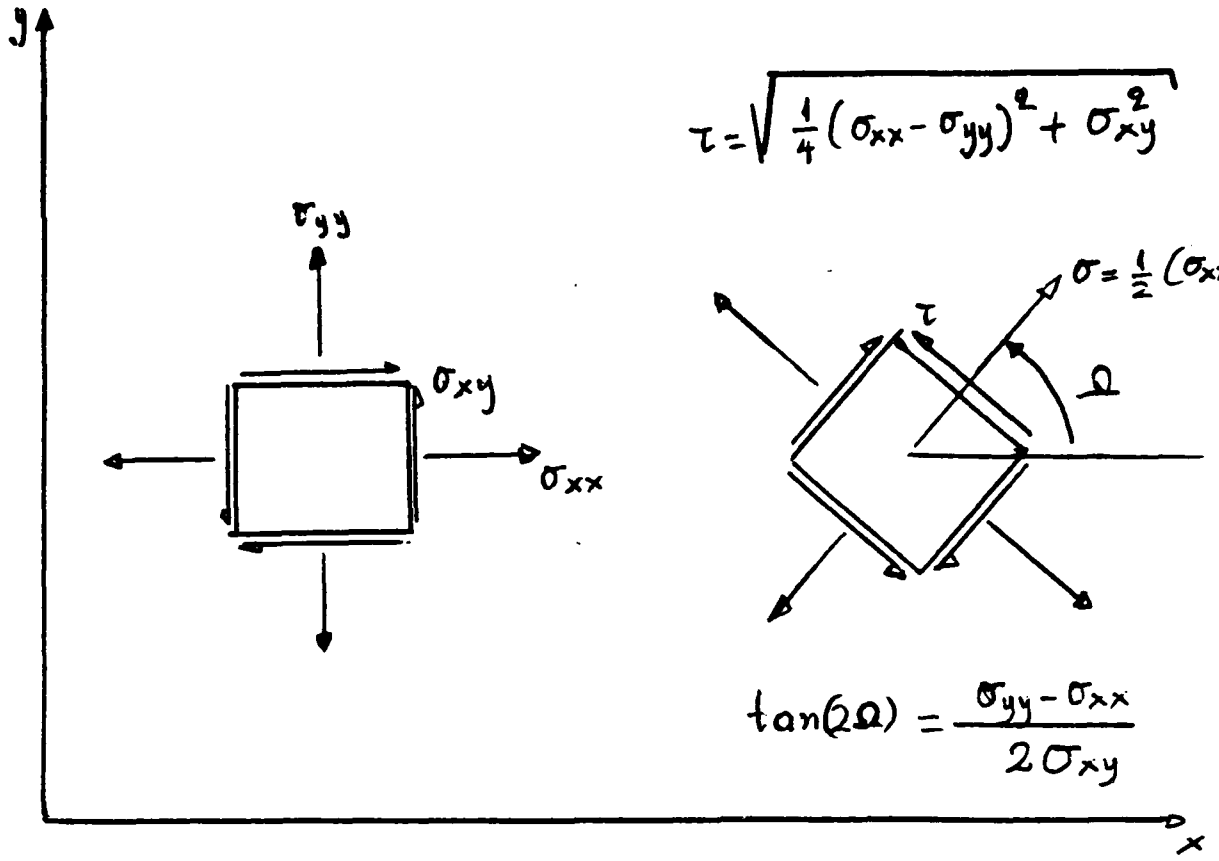

$$\tau = \sqrt{\frac{1}{4}(\sigma_{xx}-\sigma_{yy})^2 + \sigma_{xy}^2}$$

$$\tan(2\Omega) = \frac{\sigma_{yy}-\sigma_{xx}}{2\sigma_{xy}}$$

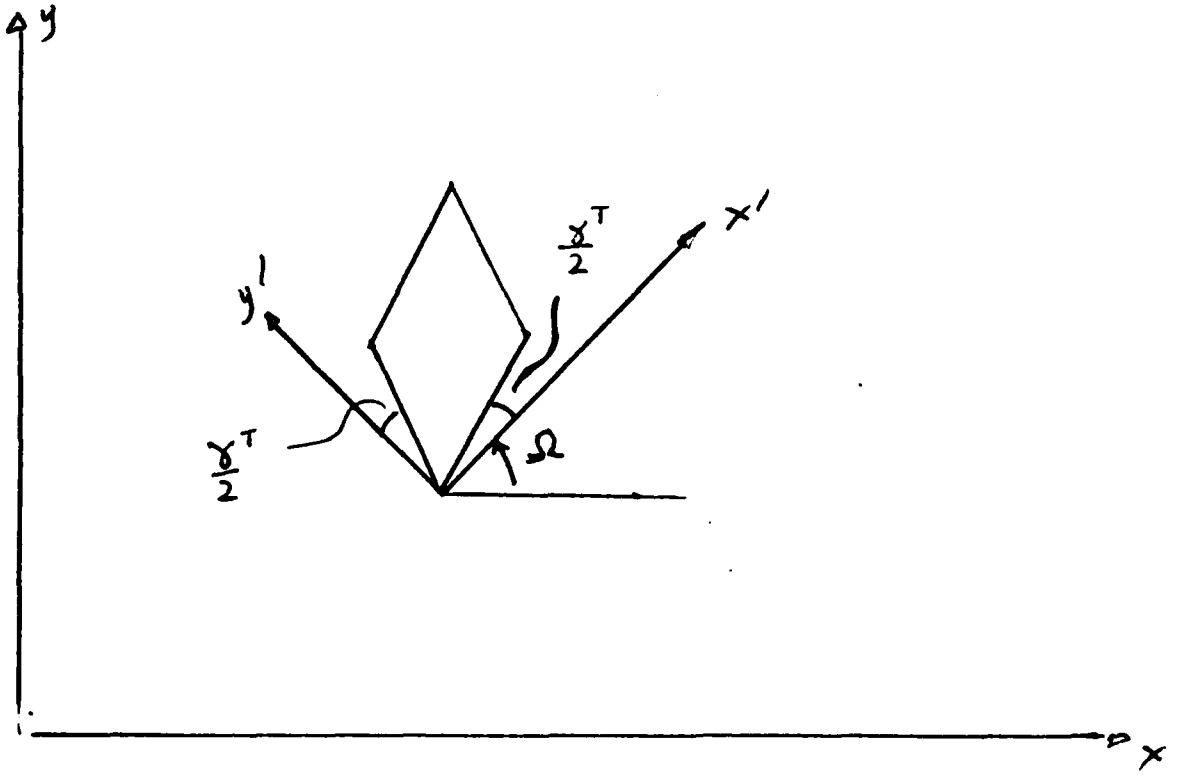

fig 1

$$R(\varphi) = \frac{8}{3\sqrt{3}} W \cos^2\left(\frac{\varphi}{2}\right)$$

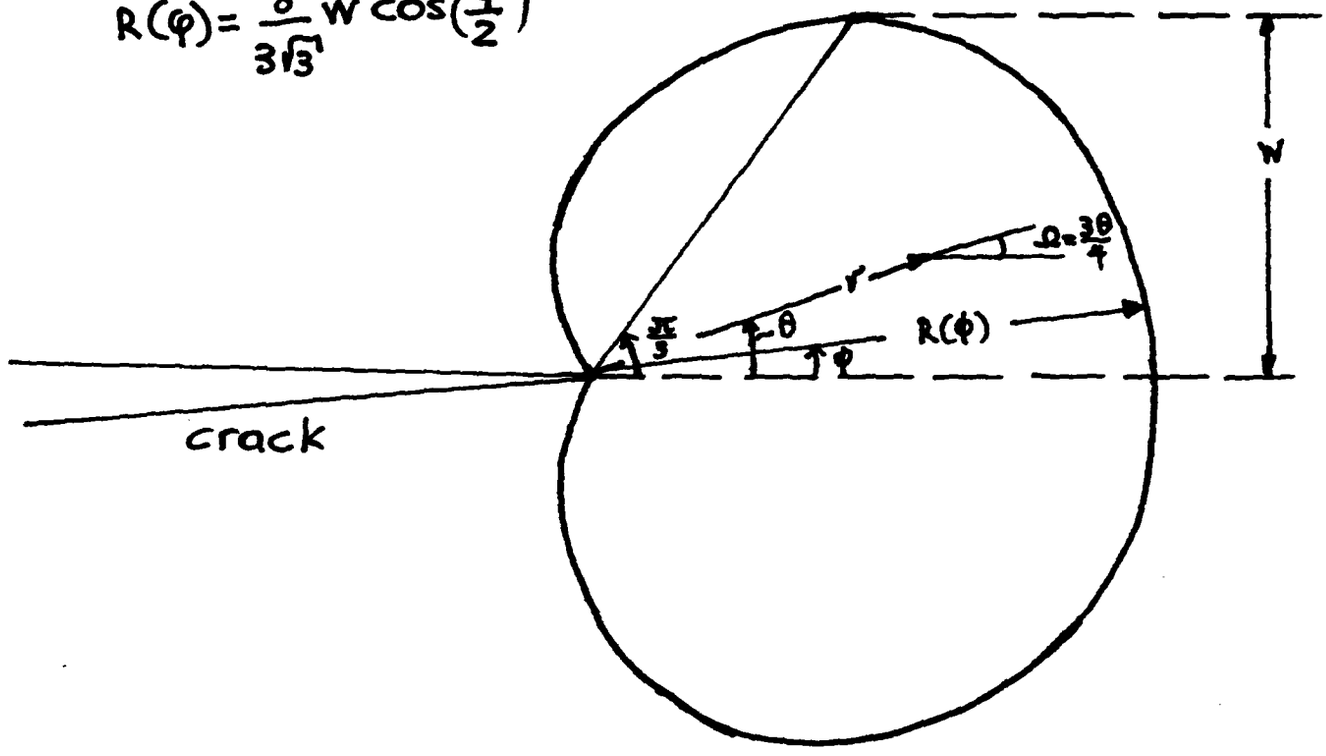

fig 2.

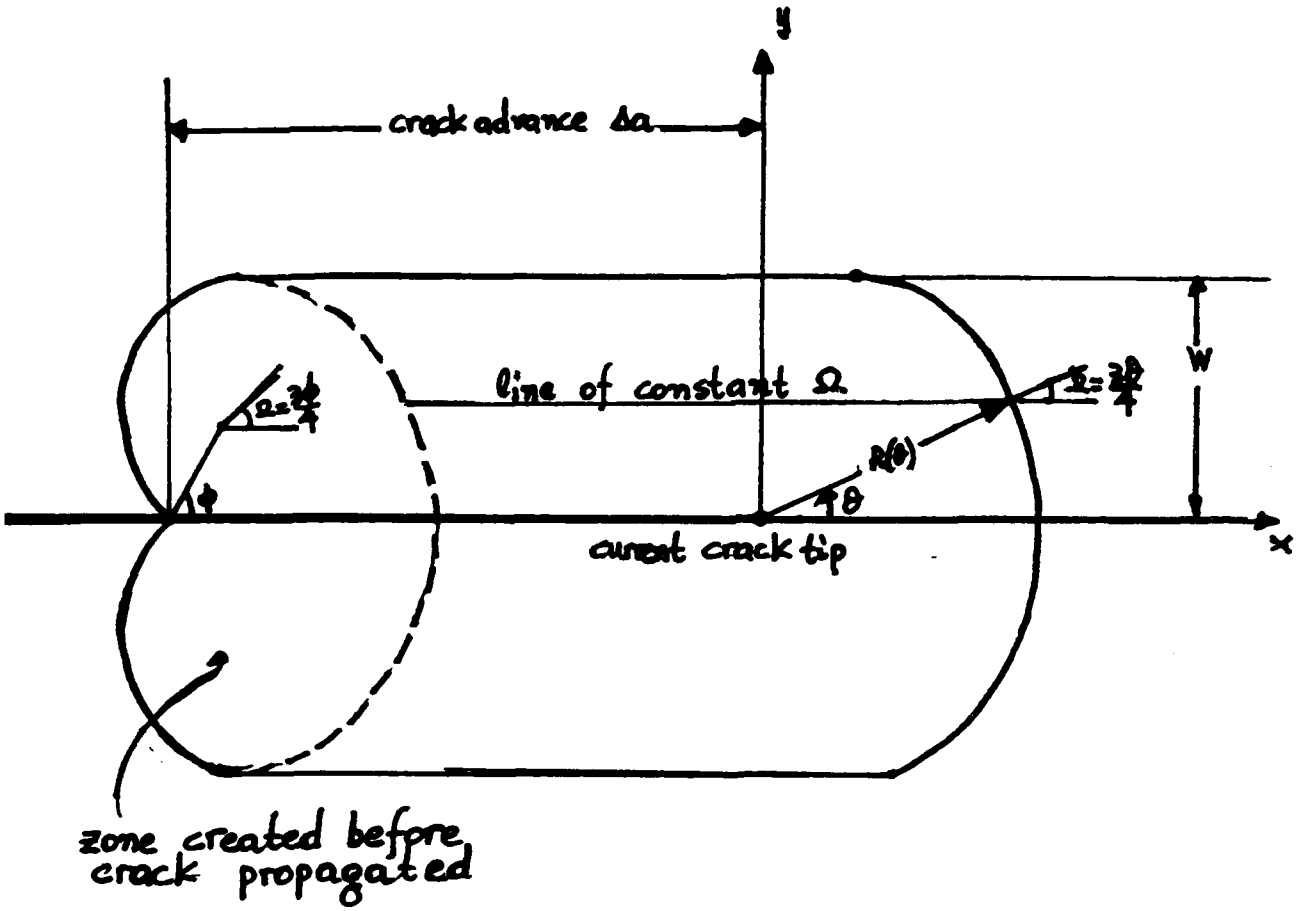
y
crack advance Δa
line of constant Ω
W
R(θ)
θ
x
current crack tip
zone created before crack propagated

fig 3

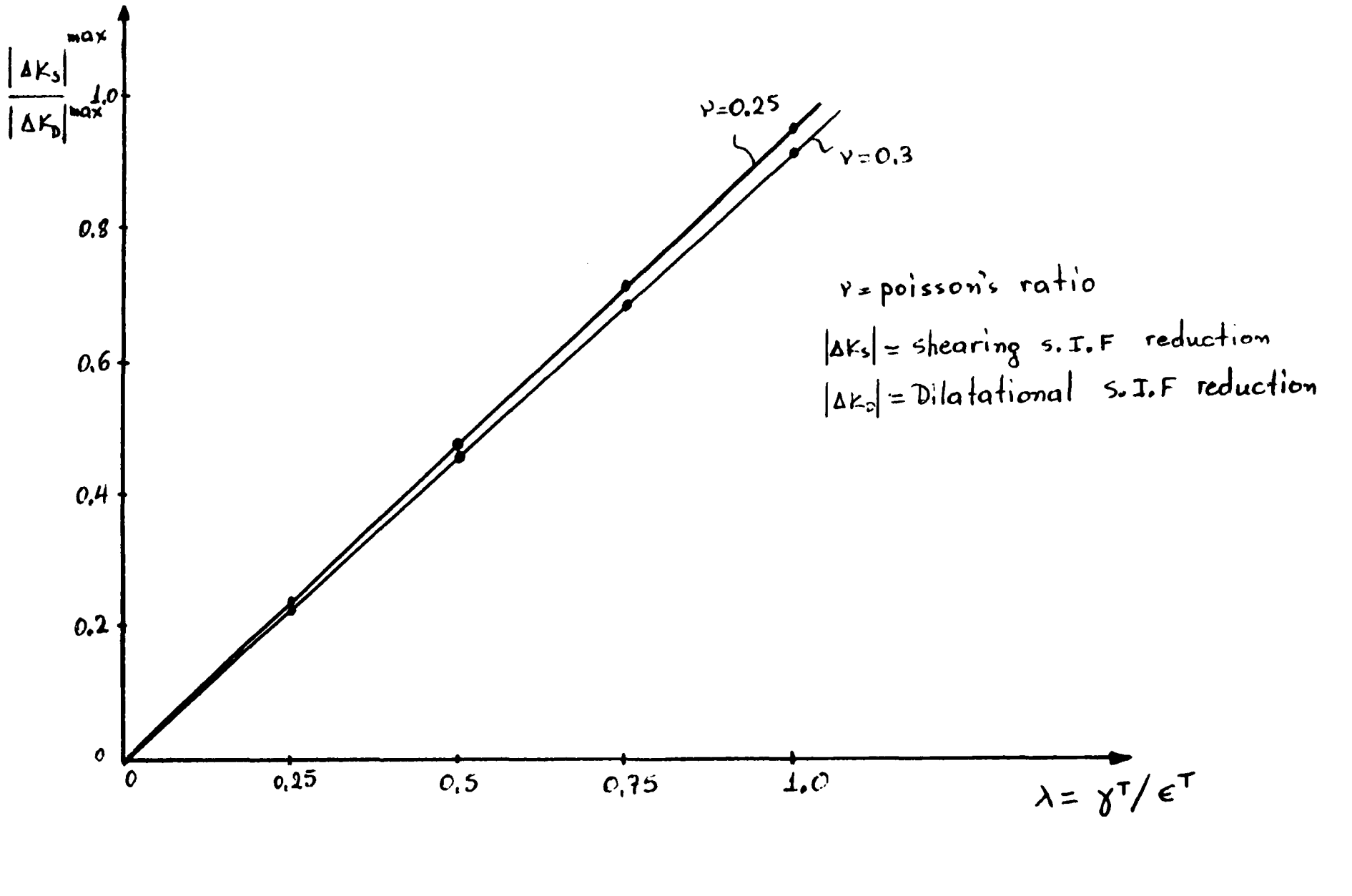
$\frac{|\Delta K_s|}{|\Delta K_D|}^{max}_{max}$
1.0
0.8
0.6
0.4
0.2
0
0
0.25
0.5
0.75
1.0
$\lambda = \gamma^T / \epsilon^T$
ν=0.25
ν=0.3
ν = poisson's ratio
$|\Delta K_s|$ = shearing s.I.F reduction
$|\Delta K_D|$ = Dilatational s.I.F reduction

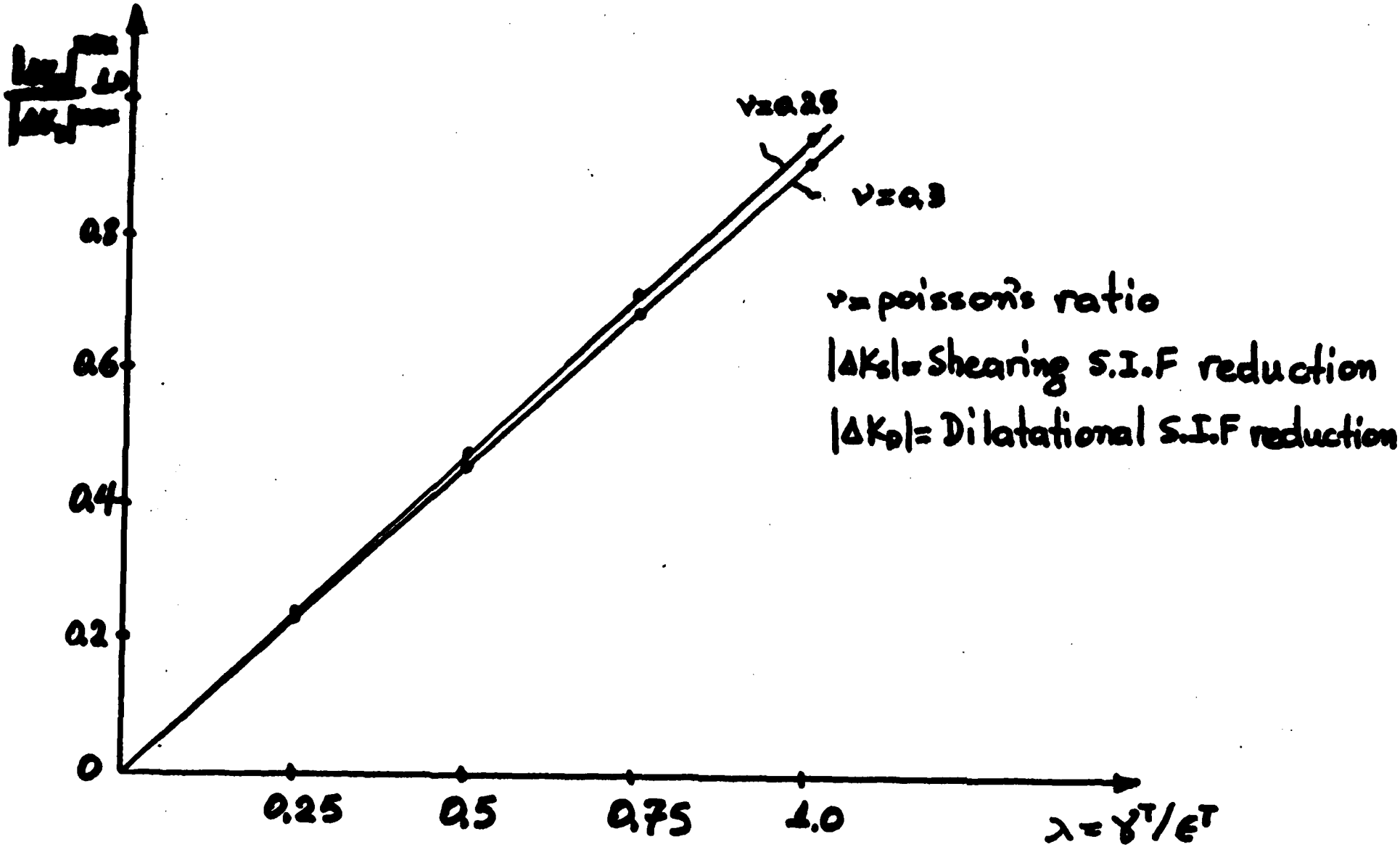
ν=0.25
ν=0.3
0.8
0.6
0.4
0.2
0
0.25
0.5
0.75
1.0
λ = γ^T/ε^T
ν = poisson's ratio
|ΔK_s| = Shearing S.I.F reduction
|ΔK_D| = Dilatational S.I.F reduction

fig 4

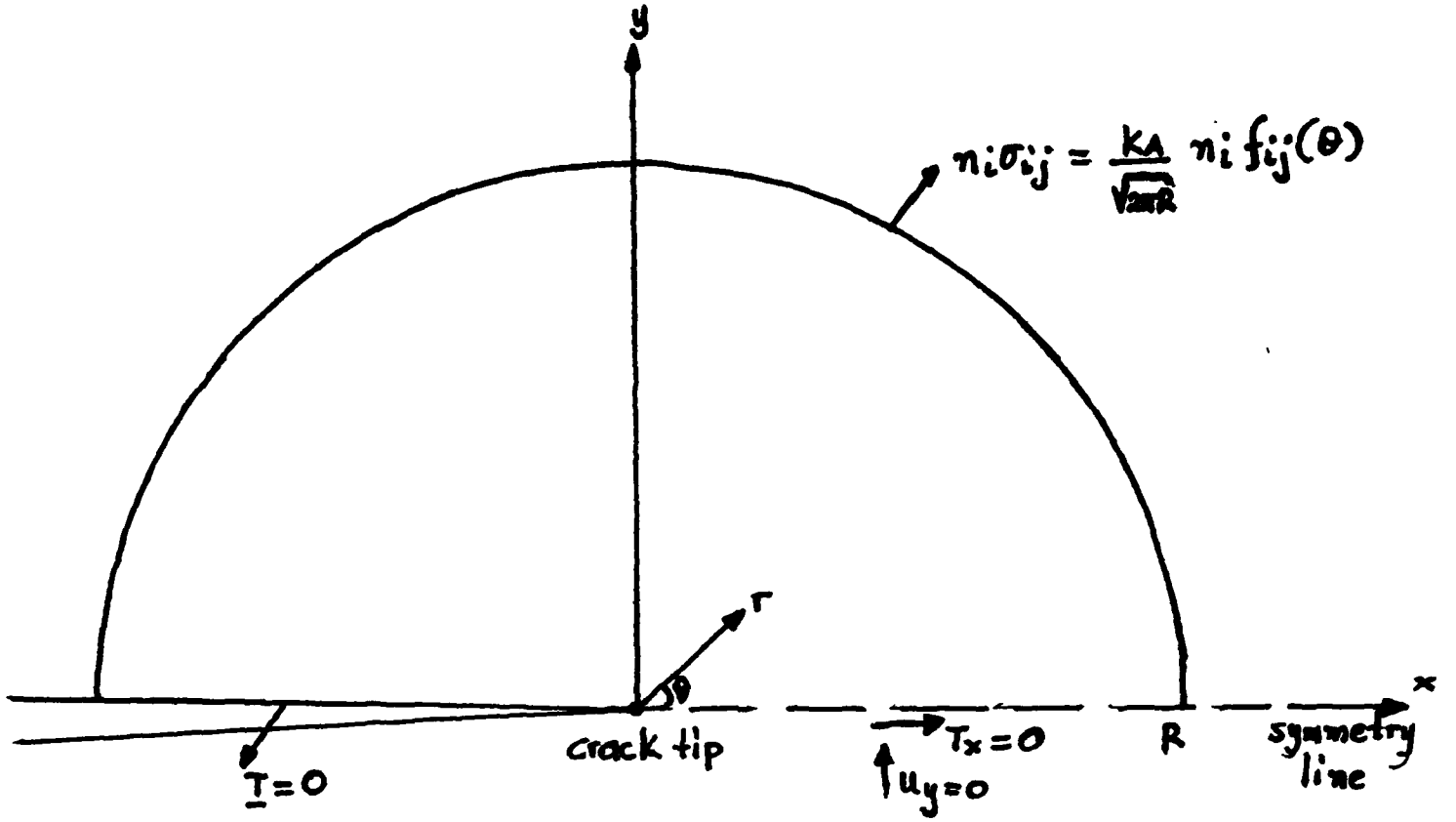
y
$n_i\sigma_{ij} = \frac{K_A}{\sqrt{2\pi R}} n_i f_{ij}(\theta)$
r
θ
x
crack tip
$T_x = 0$
$u_y = 0$
R
symmetry line
$\underline{T} = 0$

fig 5:

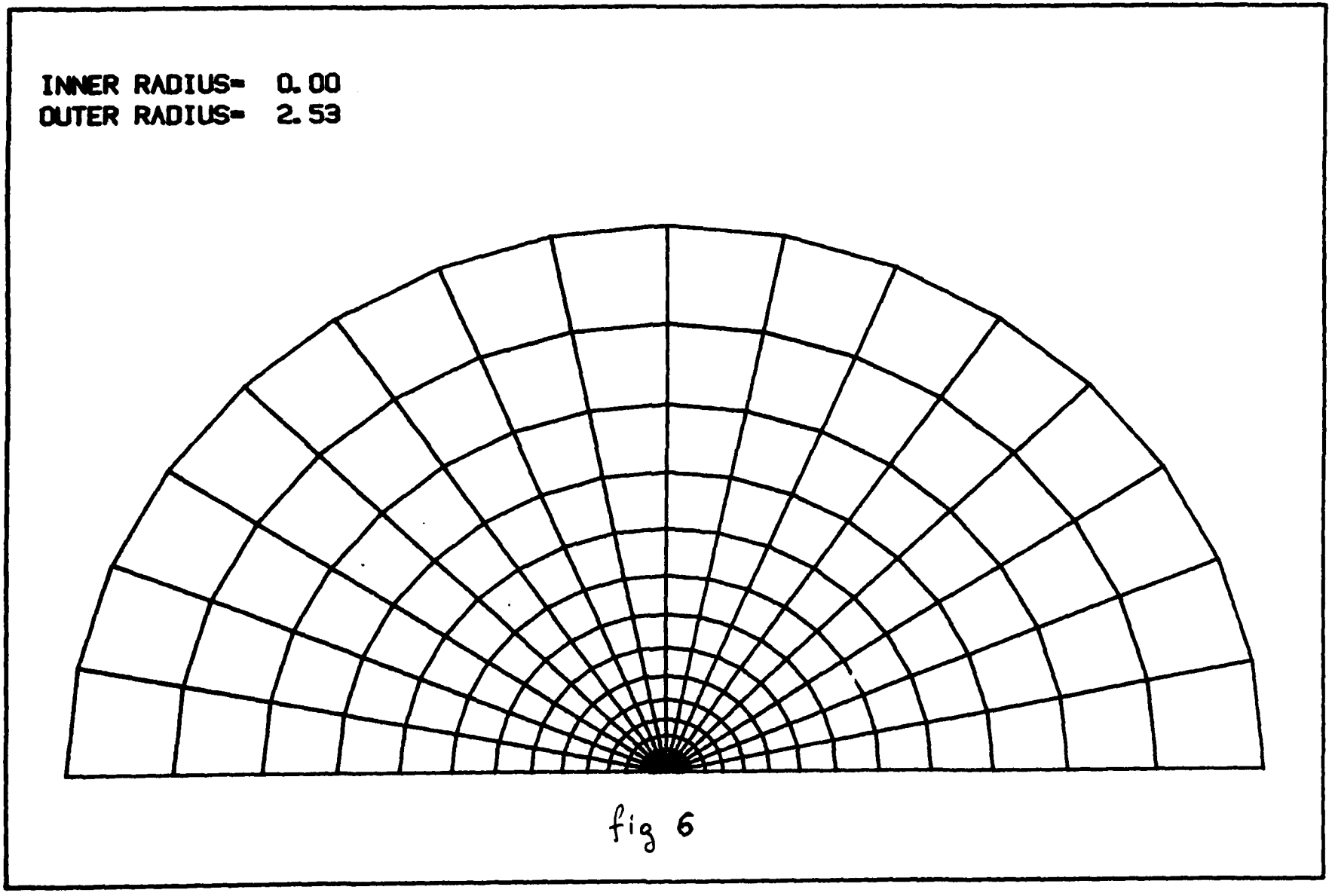

fig 6

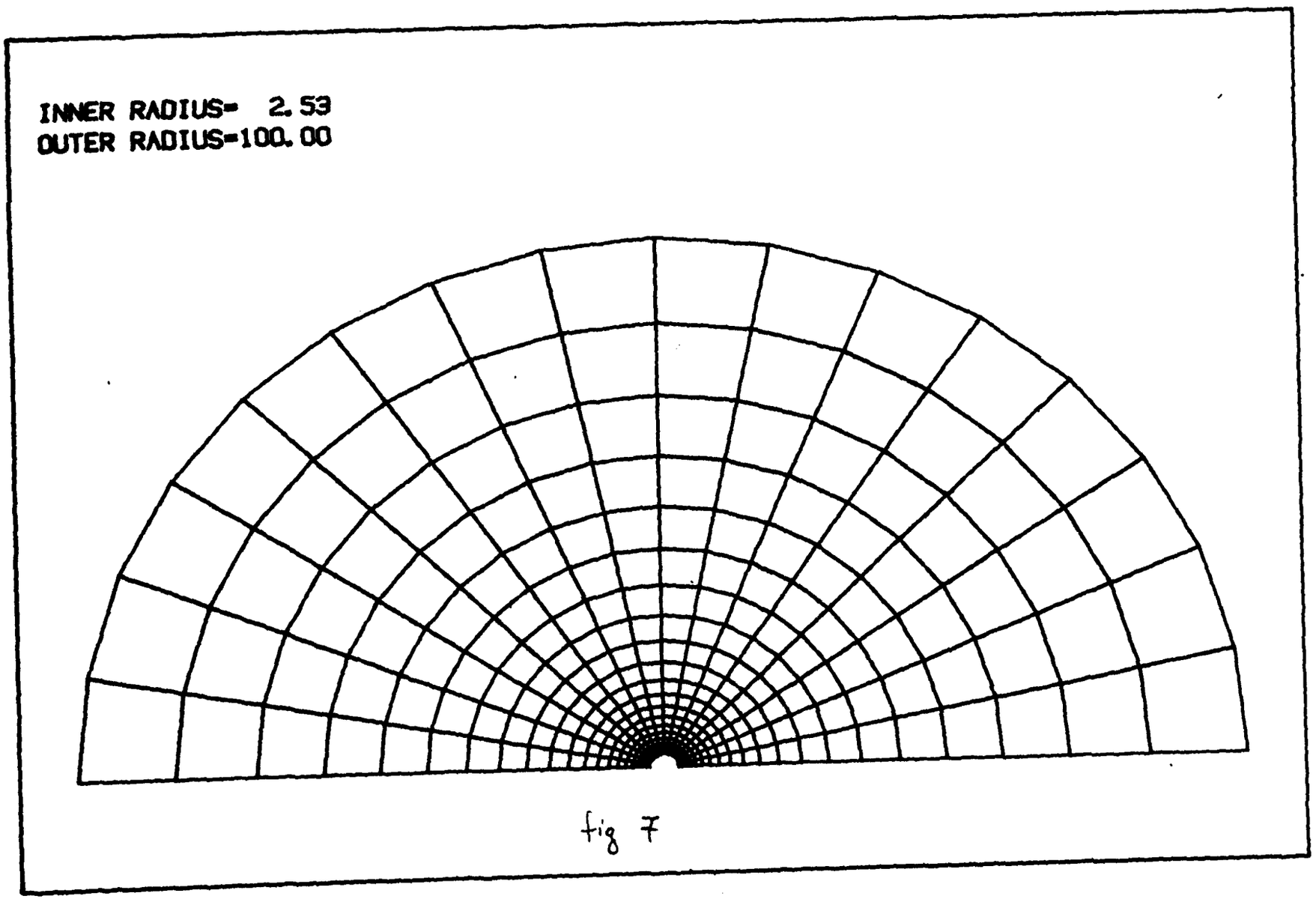

fig 7

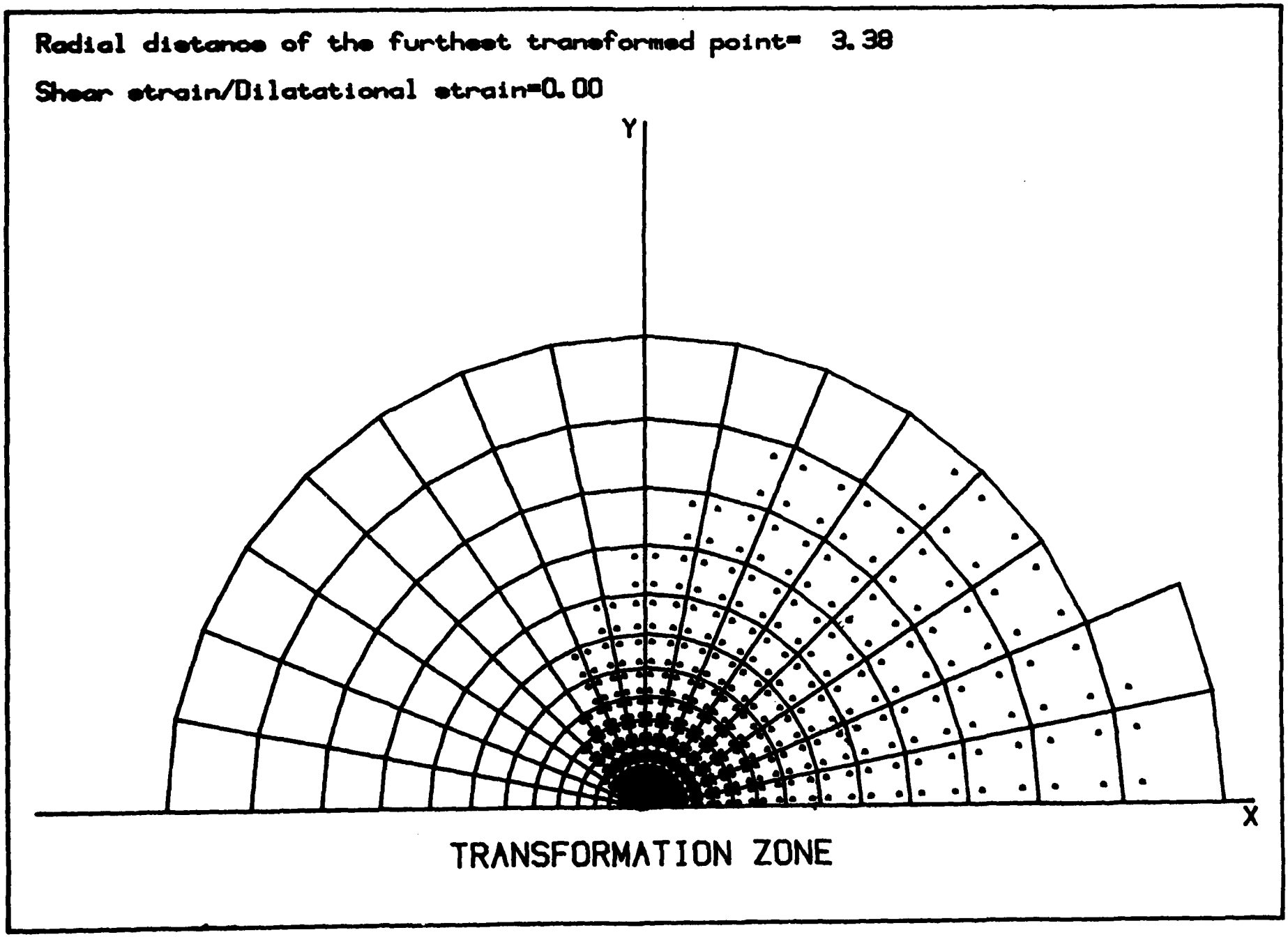
Radial distance of the furthest transformed point= 3.38
Shear strain/Dilatational strain=0.00
Y
X
TRANSFORMATION ZONE

fig 8

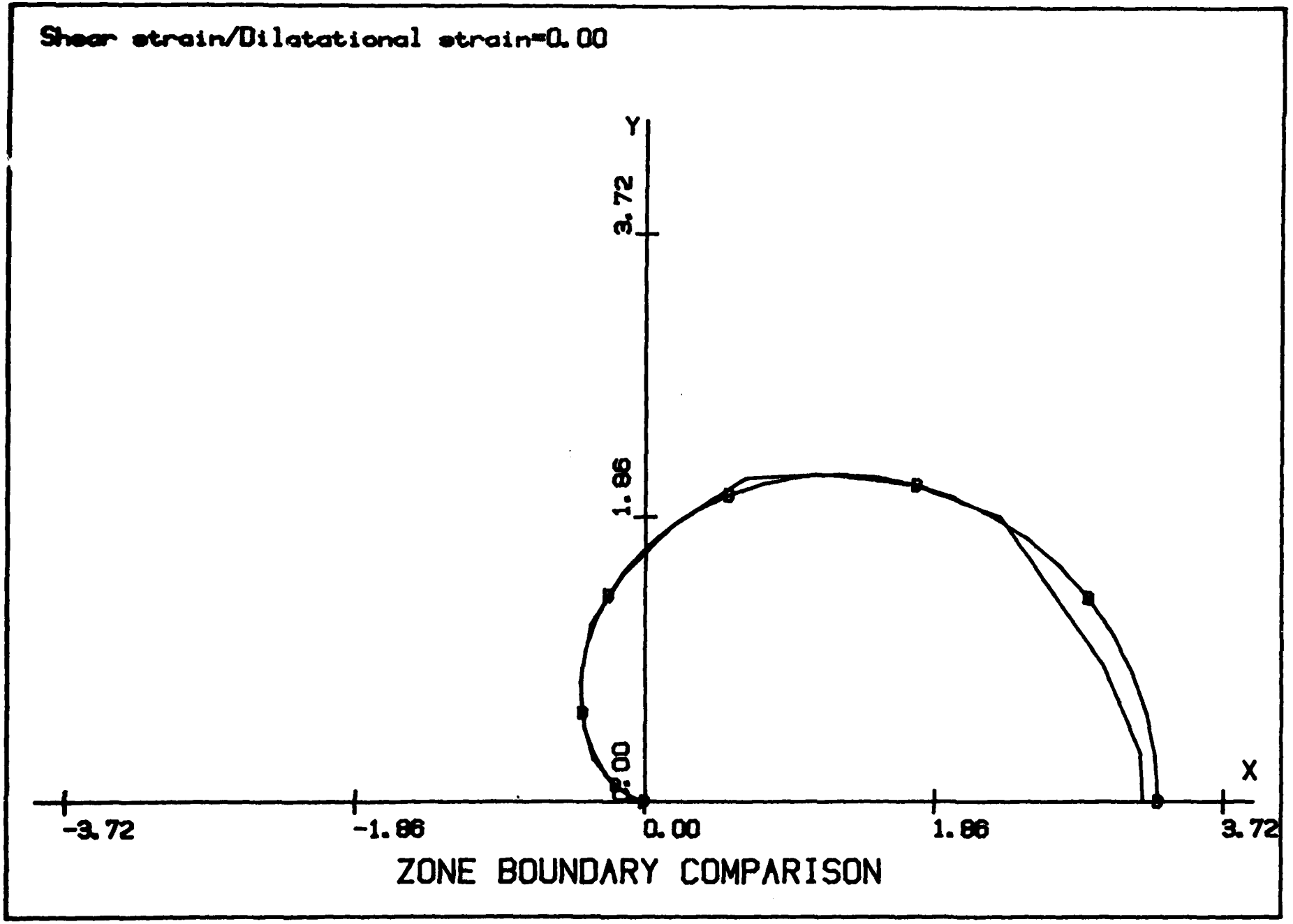
Shear strain/Dilatational strain=0.00
Y
3.72
1.86
0.00
X
-3.72
-1.86
0.00
1.86
3.72
ZONE BOUNDARY COMPARISON

fig 9

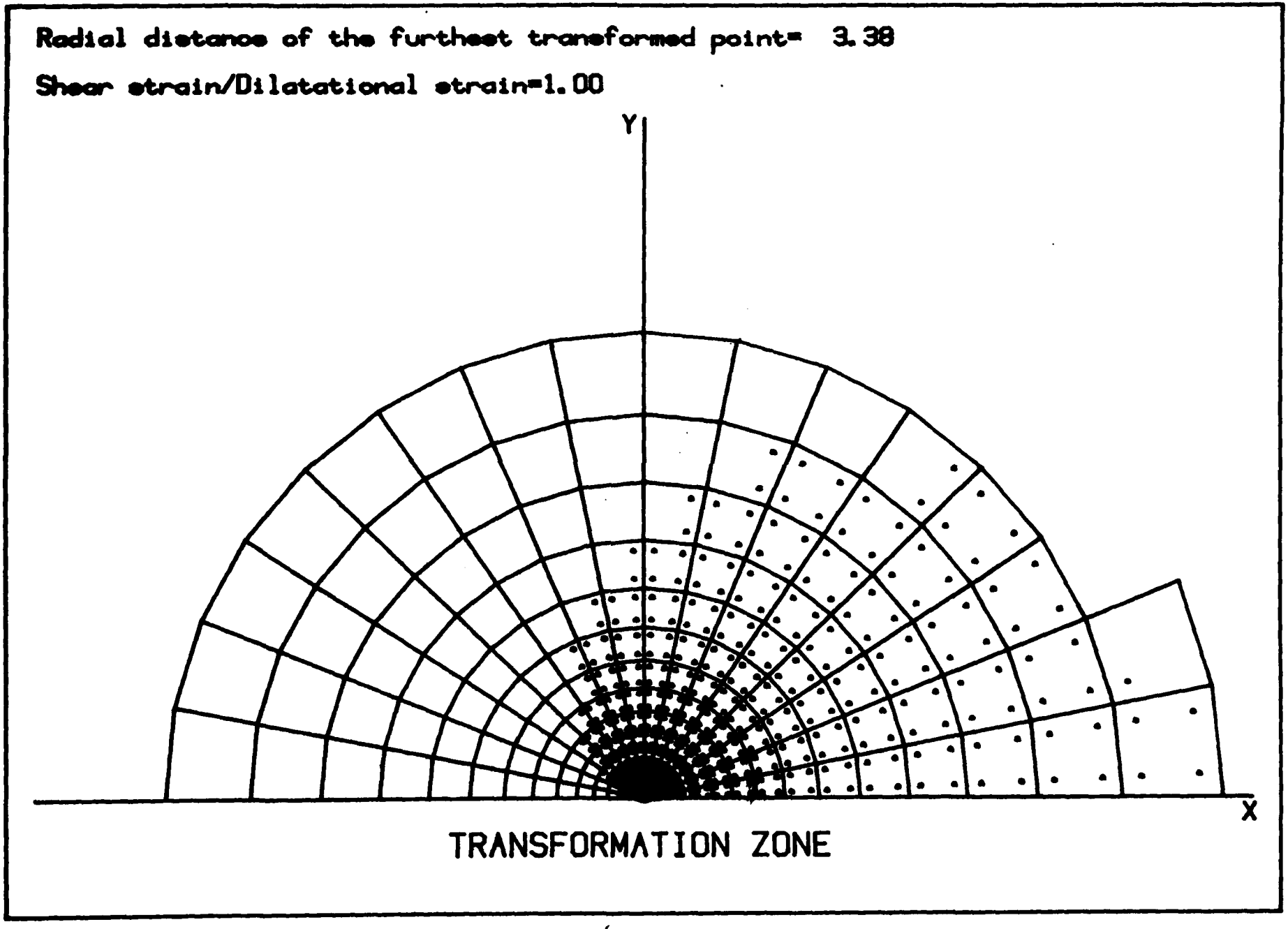
Radial distance of the furthest transformed point= 3.38
Shear strain/Dilatational strain=1.00
Y
X
TRANSFORMATION ZONE

fig 10

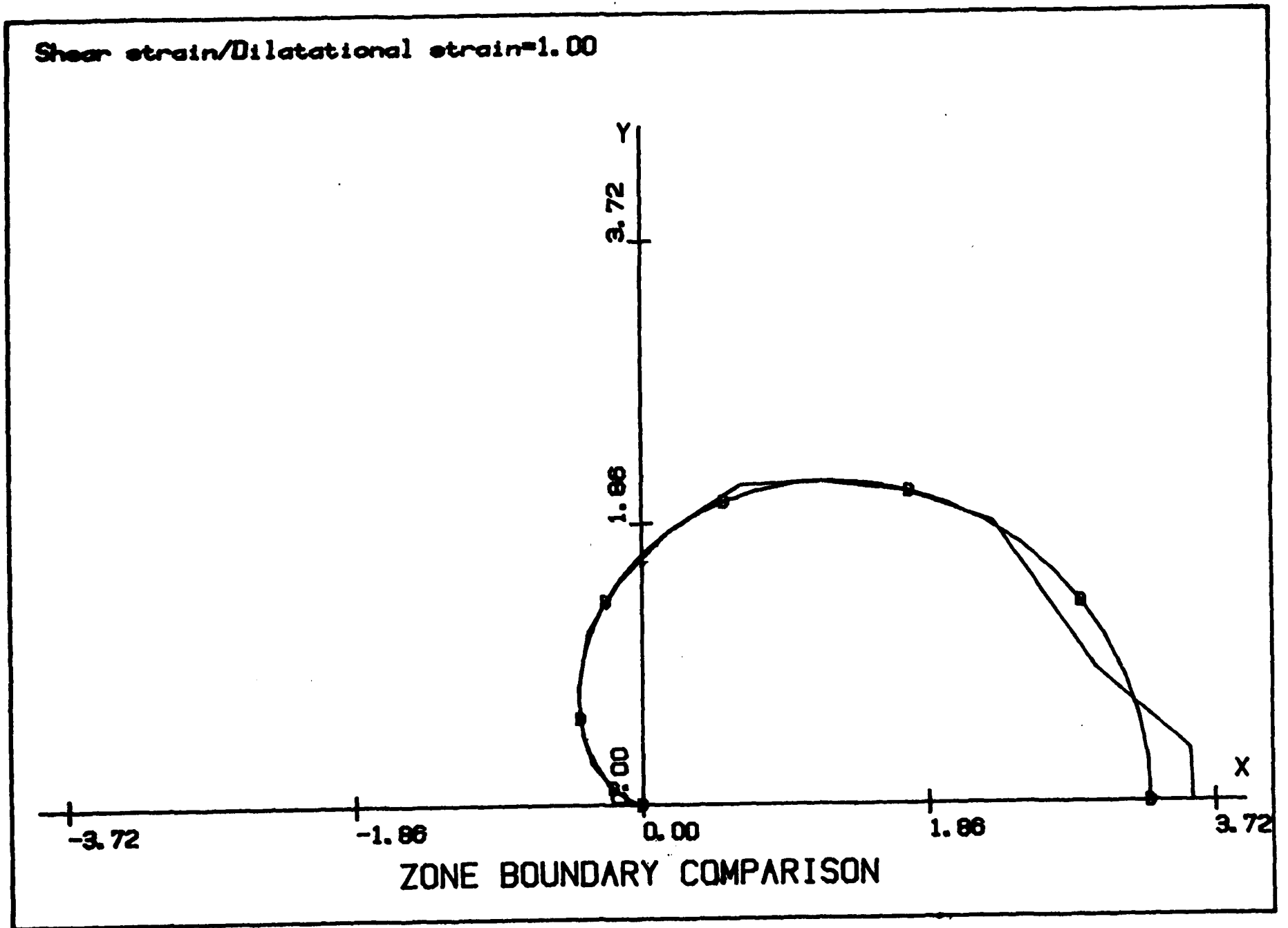
Shear strain/Dilatational strain=1.00
Y
3.72
1.86
0.00
X
-3.72
-1.86
0.00
1.86
3.72
ZONE BOUNDARY COMPARISON

fig 11

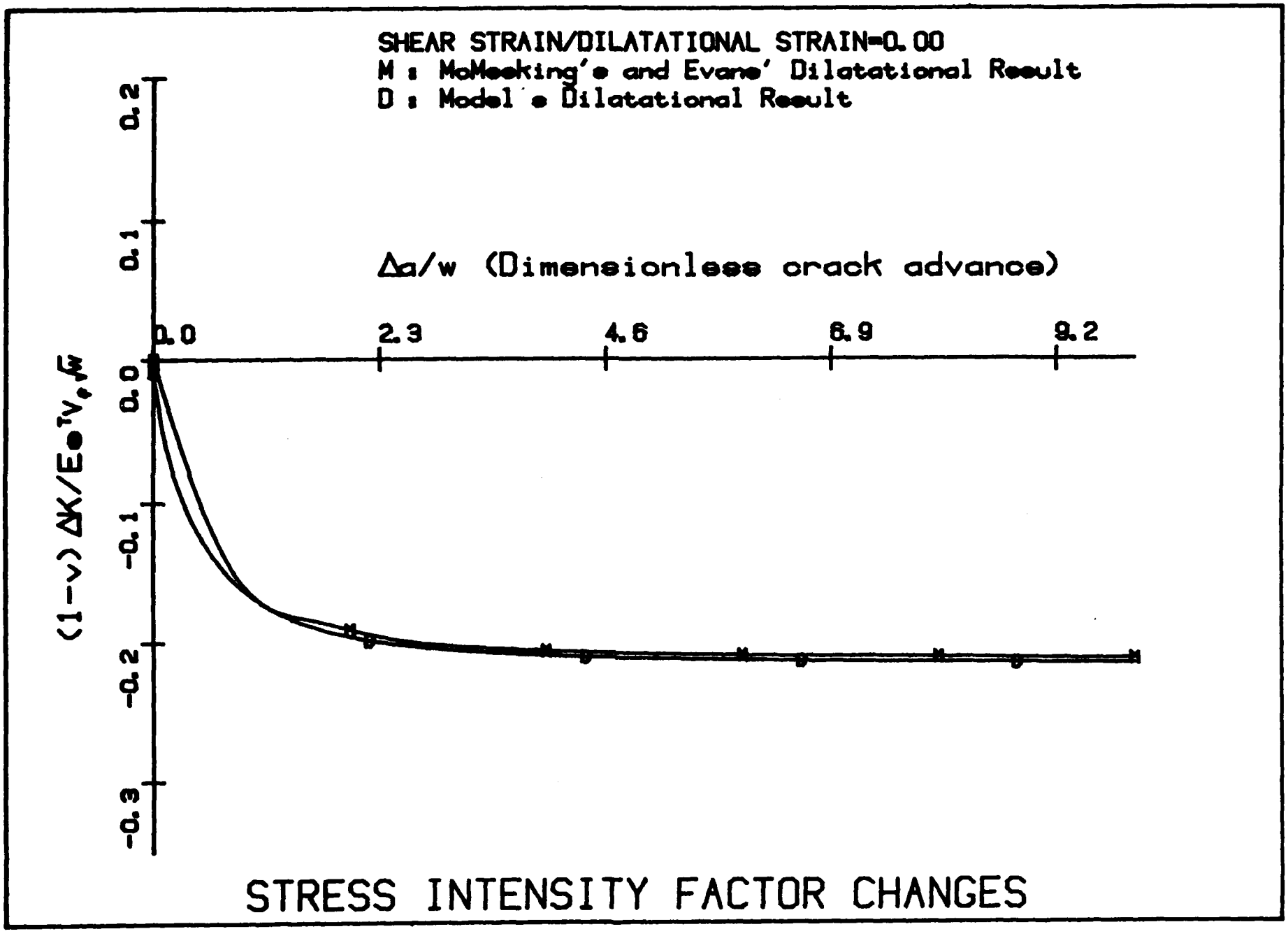
SHEAR STRAIN/DILATATIONAL STRAIN=0.00
M : McMeeking's and Evans' Dilatational Result
D : Model's Dilatational Result
Δa/w (Dimensionless crack advance)
0.0
2.3
4.6
6.9
9.2
0.2
0.1
0.0
-0.1
-0.2
-0.3
(1-ν) ΔK/E•√V•W
STRESS INTENSITY FACTOR CHANGES

fig 12

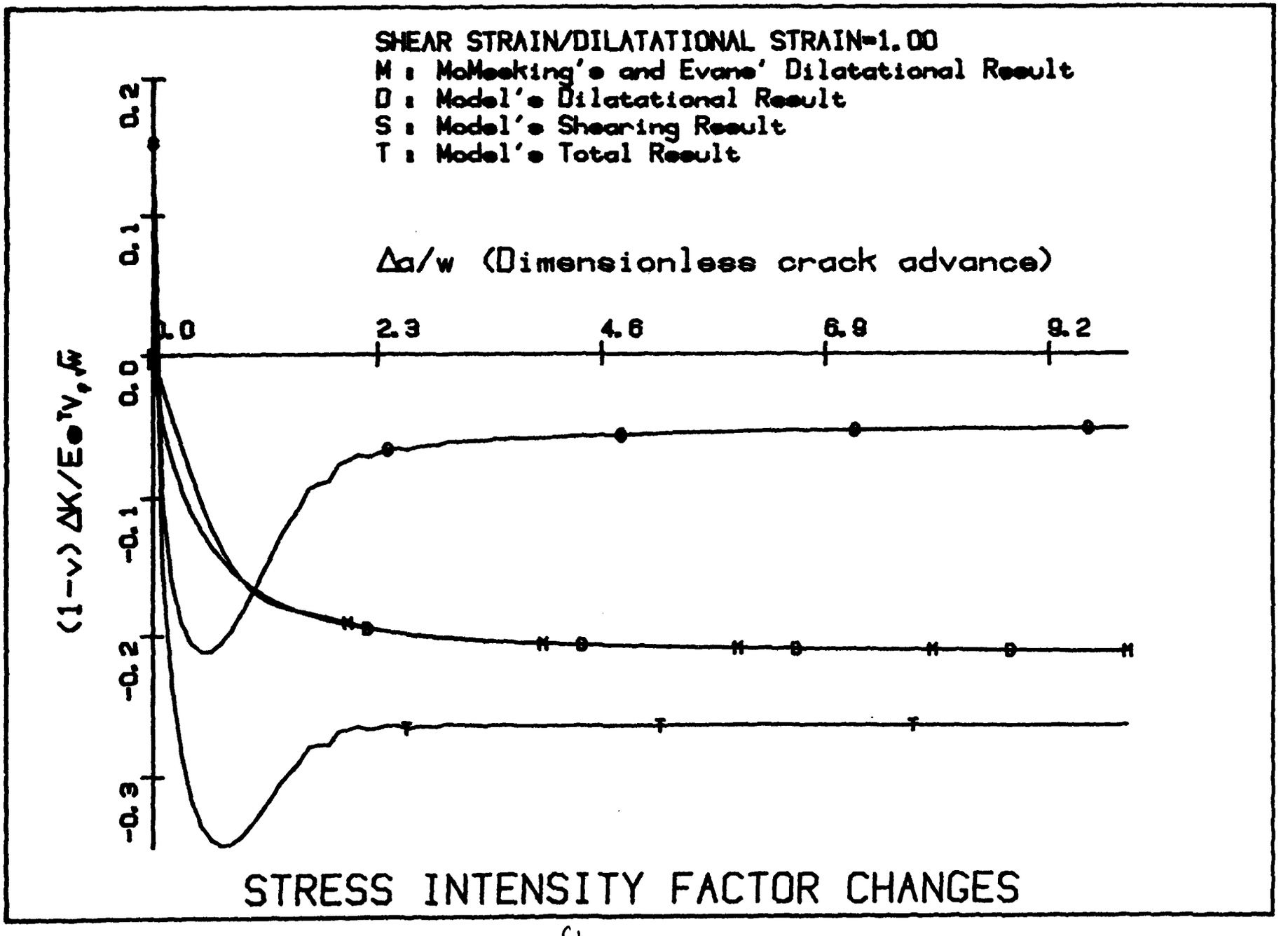
SHEAR STRAIN/DILATATIONAL STRAIN=1.00
M : McMeeking's and Evans' Dilatational Result
D : Model's Dilatational Result
S : Model's Shearing Result
T : Model's Total Result
Δa/w (Dimensionless crack advance)
0.0
2.3
4.6
6.9
9.2
0.2
0.1
0.0
-0.1
-0.2
-0.3
(1-ν) ΔK/Eε*√πW
STRESS INTENSITY FACTOR CHANGES

fig 13

END

FILMED

7-85

DTIC